Student thesis series INES nr 545

GIS-based multi-criteria analysis framework for geofence planning of dockless bike-sharing

Max Melchior Mangold

2021
Department of
Physical Geography and Ecosystem Science
Lund University
Sölvegatan 12
S-223 62 Lund
Sweden

Max Melchior Mangold (2021)
GIS-based multi-criteria analysis framework for geofence planning of dockless bike-sharing
Master degree thesis, 30 credits in *Geomatics*
Department of Physical Geography and Ecosystem Science, Lund University

Level: Master of Science (MSc)

Course duration: *January* 2021 until *June* 2021

Disclaimer

GIS-based multi-criteria analysis framework for geofence planning of dockless bike-sharing

---

Max Melchior Mangold

Master thesis, 30 credits, in *Geomatics*

Supervisors:

Pengxiang Zhao
Dep. of Physical Geography and Ecosystem Science, Lund University

Ali Mansourian
Dep. of Physical Geography and Ecosystem Science, Lund University

Exam committee:

Per-Ola Olsson
Dep. of Physical Geography and Ecosystem Science, Lund University

Acknowledgments

I want to thank my supervisors Pengxiang and Ali for their constant support and guidance who allowed me to conduct this project. I am grateful for the detailed and scrutinizing revisions of Julia and Per-Ola who followed my work from the very beginning and who many times helped me see the bigger picture. Thanks also go to Campbell and Vivi who have been a great help in the last weeks of the project. I want to express my gratitude to the experts from the City of Zürich, Pro Velo Kanton Zürich, ETH Zürich, Loughborough University and BOND Mobility AG. Without their participation in my survey, this thesis would not have been realized. I am thankful to Roll2Go AG for providing the raw bike trip data used in this research. Special thanks go to Gudrun, Johanna, and Max who provided me with superb lunch and valuable feedback on my research during the whole time of the thesis. Without them, the past five months would have been significantly more tedious and isolated. Finally, I want to thank all those people that supported me throughout my Masters both virtually via Zoom, e-mail, WhatsApp, or in person. It was a huge support to have so many great people around me.

ABSTRACT

Max Mangold: GIS-based multi-criteria analysis framework
for geofence planning of dockless bike-sharing.

Dockless bike-sharing is growing in many cities around the globe. At the same time issues related to this type of urban mobility such as illegal or improper parking behavior are becoming more frequent. The implementation of parking zones delineated by geofences has been discussed as a possible solution for these issues. This master thesis project aims to develop a GIS-based multi-criteria analysis framework for the planning of geofences for dockless bike-sharing. The proposed method combined the analytic hierarchy process and an ideal point method to select locations for geofences and their capacity in the urban space. Criteria that contribute to bike-sharing usage were determined from the literature and data to represent them was generated using GIS. A case study was conducted and its result assessed using bike trip data. The results indicate that the bike-sharing suitability computed in this study has a significant correlation with bike-sharing demand. It was shown that the presented framework was capable of planning a geofence network that had good coverage of the study area. The proposed geofences had equivalent coverage of the study area as an existing bike-sharing docking station network. The capacity computed in the case study was shown to be mostly sufficient for the demand in the study area. The method presented in this thesis can be used to plan an initial geofence network for a new dockless bike-sharing system.

Keywords: Geomatics, GIS-MCDA, multi-criteria analysis, bike-sharing, dockless, geofence, AHP, VIKOR

Contents

Table of Figures

List of Tables

Abbreviations

AHP	Analytic Hierarchy Process
COM	Density of commercial areas
EDU	Proximity to higher education (i.e. universities and colleges)
ET	Density of entertainment facilities
GIS-MCDA	GIS-based multi-criteria decision analysis
MBP	Proximity to major bike paths
MCDA	Multi-Criteria Decision Analysis
OD	Bike-trip origins and destinations
OSM	OpenStreetMap
POP	Population density
PTL	Proximity to large public transit stops and stations (i.e. train stations)
PTS	Proximity to small public transit stops and stations (i.e. tram and bus)
SP	Proximity to sports facilities and parks
WLC	Weighted Linear Combination
VIKOR	VlseKriterijumska Optimizacija I Kompromisno Resenje; engl.: Multi-Criteria Optimization and Compromise Solution

1 Introduction

Over the past two decades, bike-sharing systems have become a common mode of transportation in many cities all over the world. These systems let the user check-out a bike at one location and return it at another within the same city (DeMaio 2009; Frade and Ribeiro 2015). Bike-sharing can improve the connectivity among various modes of transit, increase the use of bicycles, help to decrease fossil fuel emissions, and have positive effects on health (DeMaio 2009; Conrow et al. 2018; Dong et al. 2019). The first attempt to launch a public bike-sharing system was carried out in the 1960s in Amsterdam. However, it was not successful and only lasted for a few days, mainly due to vandalism and theft. More recent systems aim to prevent such issues through the integration of recent technological developments like GPS tracking, smart locking devices, and smartphones (DeMaio 2009; Shen et al. 2018).

Modern bike-sharing can be put into two categories: station-based and dockless. The first operates with docking stations installed in the service area from which the bikes can be collected and to which they must be returned. The latter lets the user return the bike anywhere within the service area. Here, the bike is tracked by GPS and can be found by other users via a mobile application or website (Shen et al. 2018; Van Waes et al. 2018; Zhang et al. 2019). In comparison to station-based systems, dockless bike-sharing systems generally have lower initial costs as no stations have to be installed (Shui and Szeto 2020). They have the greatest potential for up-scaling among existing bike-sharing systems (Van Waes et al. 2018). Ma et al. (2020) showed that compared to station-based bikes, dockless bikes have a higher frequency of use and a greater usage volume.

However, the unrestricted nature of dockless bike-sharing systems is also the cause of several issues related to this technology. A major problem of dockless bikes is the parking behavior of users. Generally, dockless bikes will be more scattered within the service area, with bikes being parked in areas where there is a low demand for bike-sharing (Shui and Szeto 2020). Dockless bikes have even been found blocking sidewalks and public space due to improper parking (Liu et al. 2018; Hirsch et al. 2019; Eren and Uz 2020).

Geofencing has been discussed as a possible solution to these issues (Hirsch et al. 2019; Zhang et al. 2019; Shui and Szeto 2020). In geofencing, the location of a device is monitored by using GPS or other location services that are installed on the device. This location is checked against the coordinates of a virtual boundary that is defining the geofence (Reclus and Drouard 2009). Geofencing can be used to specify parking zones for dockless bikes. The user is then only able to lock and return the bike if they are in a parking zone. Legal frameworks that might enforce the implementation of such restrictions are currently being developed and already in place in some cities (Van Waes et al. 2018; Zhang et al. 2019).

While there are numerous studies on the location optimization of stations for station-based bike-sharing (e.g., Conrow et al., 2018; Frade and Ribeiro, 2015; García-Palomares et al., 2012; Kabak et al., 2018), there is little published research on the planning and optimization of geofences for dockless bike-sharing. The need for further research on this problem has been emphasized by Shui and Szeto (2020) and Shen et al. (2018). One of the few articles that have been published covering the topic of geofences for dockless bikes was written by Zhang et al. (2019), who used a location-allocation model to define parking zones based on big data of bike trips in Shanghai. However, this approach was only based on micro-mobility data derived from real bike trip data and does not consider other factors. It is also not applicable to a city where no such data is available. There has been extensive research on which criteria determine the bike sharing usage of a city (e.g. Faghih-Imani et al., 2014; Fuller et al., 2011; Shen et al., 2018). Kabak et al. (2018) used these criteria in a GIS-based multi-criteria decision analysis (GIS-MCDA) to compute the most suitable locations for new bike-sharing stations. In GIS-MCDA, varying weights can be assigned to the criteria before they are combined to compute the suitability of different candidate locations. By assigning weights, the varying degrees of influence on the use of bike-sharing is accounted for. To the author's knowledge, no study has employed a comparable approach to define zones for geofencing of shared dockless bikes until now.

This study aims to develop a GIS-MCDA framework for the location selection of geofences for dockless bike-sharing systems. To achieve this, the following objectives will be pursued:

- Identifying explanatory criteria for bike-sharing usage in literature
- Determining the relative importance of these criteria by implementing an analytic hierarchy process (AHP)
- Selection of geofence locations by the application of GIS-MCDA
- Determining the capacity of selected geofences by the application of GIS-MCDA
- Evaluating selected geofences with bike-usage data

The GIS-MCDA was implemented for the city of Zürich as a case study. In short, the following four research questions will be addressed:

1. What are the explanatory factors that contribute to the usage levels of dockless bike-sharing bicycles?
2. How can locations of geofences for dockless bike-sharing be selected based on explanatory factors for bike-sharing usage?
3. How can the capacity of geofences for dockless bike-sharing be determined based on explanatory factors for bike-sharing usage?
4. To what extent is the spatial distribution of demand for dockless bike-sharing in the study area covered by the geofences allocated in this study?

2 Background

This section covers related research on explanatory factors for bike-sharing usage. This literature review was used to identify the criteria for the GIS-MCDA (Table 1). The section is complemented with a synopsis of related research on dockless bike-sharing and an overview of the concept of geofencing. Furthermore, an overview of MCDA methods is provided, which is concluded by an explanation of how the MCDA procedure employed in this study was selected.

2.1 Factors contributing to bike-sharing

Various studies have investigated what factors contribute to the decision of people to use bike-sharing and bikes as means of transportation. Early studies focused mainly on the use of bicycles for commuting (Dill and Carr 2003; Krizek and Johnson 2006; e.g. Buehler and Pucher 2012). With the rise of bike-sharing, research shifted towards factors determining the use of these systems (Fuller et al. 2011; e.g. Faghih-Imani et al. 2014; Faghih-Imani and Eluru 2015; Tran et al. 2015). In more recent years, differences and parallels in usage patterns and determinants of dockless and station-based bike-sharing have been studied (McKenzie 2018; Shen et al. 2018; Ma et al. 2020).

A factor that influences cycling and bike-sharing usage is cycling infrastructure such as cycling lanes, paths, and bicycle parking (Dill and Carr 2003; Krizek and Johnson 2006; Buehler and Pucher 2012; Faghih-Imani et al. 2014; Faghih-Imani and Eluru 2015; Shen et al. 2018). Buehler and Pucher (2012) applied autoregression models on a city level and found that cities with longer bike paths have significantly higher levels of commuting by bicycle. This affirmed the results of Dill and Carr (2003) who also made a city-level comparison of cycling path density and state spending on bicycle infrastructure. Krizek and Johnson (2006) studied whether a household's closeness to cycling infrastructure would increase its probability to commute by bicycle. They found that households that have a cycling path in the proximity of 400 m or less are more likely to choose cycling as their mode of transportation. This connection between bicycle infrastructure and cycling has also been investigated with a focus on bike-sharing systems (Faghih-Imani et al. 2014; Faghih-Imani and Eluru 2015). These studies found that bike-sharing stations that have longer cycling paths in their vicinity are more frequently used than others. Similar findings were made by Shen et al. (2018) who studied the usage determinants of dockless bike-sharing in Singapore and found that proximity to longer bike paths and more frequent bike racks would be linked to higher usage of dockless bikes.

Public transit is another infrastructural factor that was found to have a significant impact on bike-sharing levels (Faghih-Imani and Eluru 2015; Tran et al. 2015; Conrow et al. 2018; Kabak et al. 2018; Liu et al. 2018; Shen et al. 2018; Wang et al. 2018; Li et al. 2020; Ma et al. 2020). Most studies investigated the effect of proximity to public transport stations on bike-sharing usage. Martin and Shaheen (2014) reason that bike-sharing has high potential to ameliorate the "last-mile problem" to get people from the trip-origin to public transit links or from those to their destination. This was supported by the results of Tran et al. (2015), who found the number of metro stations in the vicinity

of a bike-sharing station to be significantly positively correlated with bike-sharing levels. Similar findings arose in the research of Faghih-Imani and Eluru (2015). Their results indicate that regular bike-sharing users tend to use bike-sharing in combination with public transit. Wang et al. (2018) also found that bike-sharing stations in areas with a higher density of public transit stations have higher bike-sharing usage. This relationship has also been shown for dockless bike-sharing systems. Shen et al. (2018) stated that "[…] usage of dockless bikes is most concentrated around [metro] stations". Correspondingly, Liu et al. (2018) found that 60% of the dockless bikes in their case study were located within a maximum distance of 1 km from the nearest metro station. Another study showed that high density of bus and metro stations significantly decreases the time periods in which dockless bikes are not used (Li et al. 2020).

Apart from infrastructure there are also other built environment facilities that affect bicycle usage. Bike-sharing activity is higher in proximity to the central business district and other commercial areas such as shopping centers (Kaltenbrunner et al. 2010; Faghih-Imani et al. 2014; Liu et al. 2018). This was first studied for station-based bike-sharing systems (Kaltenbrunner et al. 2010; Faghih-Imani et al. 2014) and later also demonstrated for dockless bike-sharing systems (Liu et al. 2018). The last study analyzed the correlation between the number of bikes in an area and various explanatory variables. Their results indicate that distance to the nearest business center has the strongest influence among the studied variables, with a Pearson correlation coefficient of -0.79.

Several studies tried to evaluate the effect of entertainment facilities on bike-sharing usage. These efforts focused mostly on the density of restaurants and other food services (Faghih-Imani et al. 2014; Faghih-Imani and Eluru 2015; Wang et al. 2018; Li et al. 2020). Ma et al. (2020) and Tran et al. (2015) additionally considered other entertainment facilities like cinemas. They observed that dockless bike-sharing has a positive relationship with entertainment facilities whereas station-based bike-sharing has a negative correlation. However, the relationship with station-based bike-sharing seems to be less clear as other studies have found a positive relationship (Faghih-Imani et al. 2014; Faghih-Imani and Eluru 2015; Tran et al. 2015; Wang et al. 2018).

Green space and parks have less often been studied as a determinant for bike-sharing activity. To the author's knowledge, only two studies, namely Faghih-Imani and Eluru (2015) and Wang et al. (2018), considered this factor in their analysis of bike-sharing patterns. Both studies found that parks attract more bike-sharing trips for recreational use whereas no effect on regular commuter use was identified. Faghih-Imani and Eluru (2015) also identified a pattern of higher bike-sharing usage around parks on weekends compared to weekdays.

There is similarly little research published on the effect that sports facilities have on bike-sharing activity. Wang et al. (2018) observed a positive relationship between the area of recreational space around bike-sharing stations and the number of bike-sharing trips generated by stations. This trend was observed for most age groups. In their case study in Barcelona, Tran et al. (2015) found that most

bike-sharing trips in the afternoon could be explained by proximity to recreational facilities such as sports amenities.

The factors that were outlined until now cover the built environment. However, there are also demographic and socio-economic variables that might influence bike-sharing levels. The factor among these that has been most thoroughly examined is population density (Faghih-Imani et al. 2014; Martin and Shaheen 2014; Faghih-Imani and Eluru 2015; Tran et al. 2015; Wang et al. 2018; Li et al. 2020). All these studies share the finding of higher bike-sharing activity in areas of higher population density. Most of the studies studied bike-sharing usage of station-based systems except for Li et al. (2020) who conducted an empirical study of dockless bike-sharing. They showed that bikes have a shorter stop duration (i.e. the time in which a bike is not being used) in areas of higher population density. It is noteworthy that the relationship varies both temporally and between generations. Faghih-Imani and Eluru (2015) observed that the trend is reversed in the morning when more trips originate from suburban areas which have lower population densities. Wang et al. (2018) found that all age groups except for those aged between 30 and 53 exhibit higher levels of bike-sharing use in areas of higher population density.

Proximity to universities has been studied as a driver for higher cycling and bike-sharing activities (Kaltenbrunner et al. 2010; Faghih-Imani et al. 2014; Frade and Ribeiro 2015; Wang et al. 2018; Li et al. 2020). This factor is related to demography as it is more likely to be strongly influenced by students and thus younger people. Of the studies mentioned, only Faghih-Imani et al. (2014) and Wang et al. (2018) explicitly investigated the relationship of proximity to nearest university and bike-sharing usage levels. Both studies found that a significantly larger number of bike-sharing trips were generated at stations closer to universities. Most other publications that mention this relationship are case studies in which a potential positive correlation of shorter distance to the nearest university and bike-sharing activity was discussed (Kaltenbrunner et al. 2010; Frade and Ribeiro 2015; Li et al. 2020). This relationship is supported by the work of Dill and Carr (2003), who found that university towns have higher levels of cycling. Similarly, a Canadian study concluded that students are more likely than other population groups to use bicycles to move around in a city (Butler et al. 2007). Based on these findings it can be assumed that cycling levels around university campuses are potentially higher than in other parts of a city.

2.2 Research on dockless bike-sharing and geofencing

Up till now, research on dockless bike-sharing has mostly focused on two aspects, the explanation of bike usage patterns and the rebalancing of shared bikes. Several studies have suggested using geofencing to solve parking and rebalancing issues related to dockless bike-sharing (Hirsch et al. 2019; Zhang et al. 2019; Shui and Szeto 2020). However, only two studies aimed at developing a method for geofence planning (Cheng et al. 2019; Zhang et al. 2019). In this section, related research

on dockless bike sharing, the concept of geofencing and the possible design of such a system for dockless bike-sharing will be outlined.

An early study on rebalancing was published by Pal and Zhang (2017) who developed an algorithm for the planning of real-life static rebalancing of dockless bikes. Li et al. (2020) studied bike-sharing utilization and its explanatory factors. Two other articles also studied explanatory factors of spatio-temporal usage patterns of dockless bike-sharing and compared it to those of station-based bike-sharing (McKenzie 2018; Ma et al. 2020). Liu et al. (2018) studied factors affecting bike distribution and developed an inference study for the planning of a bike-sharing system in a new city. To the author's knowledge, Zhang et al. (2019) and Cheng et al. (2019) are the only studies that proposed methods for geofence planning for dockless bikes. In these studies, geofence locations were derived from usage data of dockless bikes. Hence, these approaches can only be applied where such data is available. Zhang et al. (2019) themselves concluded that other explanatory factors can be included in the geofence planning too.

Geofencing is based on monitoring a device's location using location services such as GPS. The location is frequently sent to a control server which checks it against the coordinates of a virtual boundary that defines the geofence. There are different fields of application such as logistics, security, and fleet management. The shape of a geofence zone can vary. In a simple approach, a buffer around point coordinates is defined and the system notes when a tracked device enters or leaves this buffer zone. However, it is also possible to define more complex shapes so that any kind of polygon can be used as a geofence (Reclus and Drouard 2009).

In this study, geofences will refer to zones that restrict the parking of dockless, shared bikes. In a system where such geofences are implemented users will only be able to lock and return the bike if the location-monitoring approves that they are within a geofence. Such zones can be regarded as virtual bike sharing stations with the main difference that no built structures are required. Zhang et. al. (2019) specified a size of 2 times 15 m for the geofences created in their study. Two examples of cities in which such a type of geofencing is used are Kiel, Germany and Canberra, Australia (Figure 1). Legal frameworks that enforce the implementation of geofence restrictions for dockless bike-sharing are currently being developed in many cities (Van Waes et al. 2018; Zhang et al. 2019).

2.3 Multi-criteria decision analysis

Decision-makers use Multi-criteria Decision Analysis (MCDA) to structure and process large amounts of complex information. This is particularly useful if more complex factors that all affect decision making have to be considered. MCDA makes it possible to deal with the different criteria that affect the outcome of decisions in a systematic and consistent manner (Hwang and Yoon 1981). MCDA methods can be grouped in two classes that are distinguished by the number of alternatives they can handle. The first class is commonly referred to as multi-attribute decision methods and approaches in that class can deal with a finite number of alternatives to decide from. Methods

Figure 1. Parking zone for dockless bike-sharing in Canberra, Australia. Note the marking on the ground and the lack of any built structures. Source: https://commons.wikimedia.org/wiki/File:Dockless_bike_parking_area_on_Lonsdale_Street_August_2018.jpg (CC BY-SA, Accessed on May 18, 2021)

belonging to the second class on the other hand, can deal with an infinite number of alternatives and are usually called multi-objective decision methods (Hwang and Yoon 1981). In this study, a set of geofence locations shall be selected from a large but finite dataset of candidate locations. Multi-objective decision methods are also called *a posteriori* since they involve decision makers after the analysis was conducted. Decision makers are then asked to place appropriate sites from a suitability map. However, the approach followed in this study aims to combine knowledge of several different experts from varying backgrounds. Gathering all of these experts together to select a large number of locations would not be feasible. Therefore, multi-attribute methods were selected where experts are involved in the early stages of the analysis. The term MCDA will in the following be used exclusively for multi-attribute decision analysis. For an explanation of how the candidate locations were selected, refer to section 3.6.

The two core concepts that are part of most MCDA techniques are scoring and weighting (Eastman et al. 1993). Scoring refers to the assignment of a score value to each criterion of the alternatives. The score value reflects the performance or suitability of an alternative with regards to the criterion. By weighting, the influence of the different criteria relative to each other can be reflected in the decision-making process. MCDA problems can be very complex. Thus it can be necessary to acquire expert knowledge to assign weights to the criteria. Many different MCDA methods exist. Among the most common methods in GIS-MCDA are linear additive modeling (e.g. linear weighted combination), the analytic hierarchy process, ideal point methods (e.g. VIKOR), and outranking (e.g. ELECTRE; Malczewski, 2006). However, there is no single method that consistently yields the best results and which method to apply depends on the decision problem (Guitouni and Martel 1998). Wątróbski et al. (2019) developed a framework to select the appropriate MCDA method for a given decision

problem independent of the field of research. It bases the method selection on four main problem descriptors that correspond to the following questions:

1. Will criteria weights be taken into account?
2. What is the scale of the criteria performance (i.e. quantitative or qualitative)?
3. Is the problem characterized by uncertainty?
4. What is the desired outcome of the method (i.e. selection, classification, ranking and selection, classification and selection)?

This framework was used to select the appropriate MCDA method for this study. Refer to section 3.2 for the problem descriptors of this study and for the method selection.

3 Methodology

The methodology of this study can be divided into four main parts (Figure 2). Firstly, criteria that influence bike-sharing demand and parking suitability were determined using existing literature. Secondly, an AHP was conducted to assess the level of influence of the individual criteria and to derive weights (Kabak et al. 2018). In addition to that, spatial data to represent the criteria was attained and criteria layer were computed. Thirdly, the GIS-MCDA framework was implemented. This entailed two subsequent analyses: (1) the ranking of the candidate locations using VIKOR, and (2) the selection of the final locations using a location-selection that included a minimum spacing constraint between geofences. In this step the geofence capacity was also derived from the VIKOR suitability ranking and the existing infrastructure available at the geofence location. Additionally, a suitability map was created by combining the criteria using a weighted linear combination (Eastman et al. 1993). The criteria were standardized before the combination was done (Keeney 1992). The suitability map served as visualization guidance to select an appropriate dataset for the candidate locations. Lastly, the resulting geofence was evaluated by studying the degree to which the actual bike-sharing usage is covered by the geofence. For this, the bike ride data that was acquired for Zürich was used and statistically analyzed.

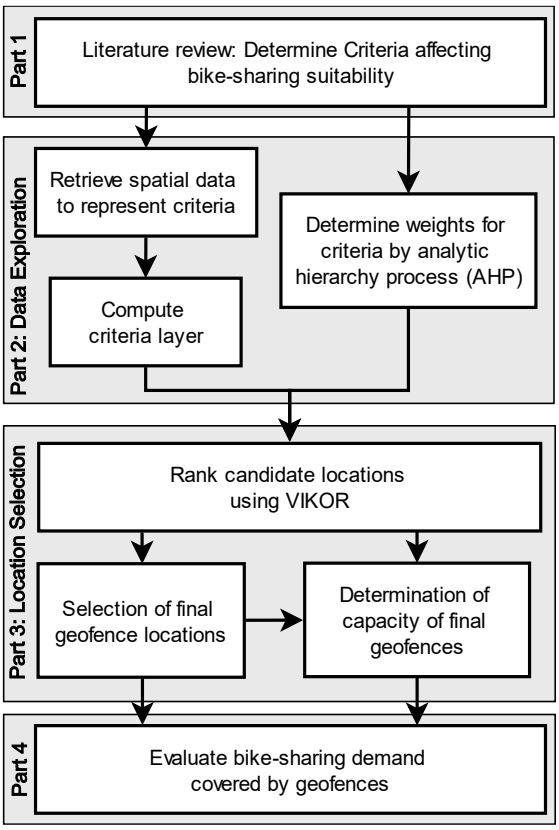

Figure 2. Flowchart of methodology.

3.1 Data & Study area

The case study was conducted for the city of Zürich, Switzerland. Zürich is the largest Swiss city with a population of over 435 000 Inhabitants (Stadt Zürich 2021; Statistik Stadt Zürich 2021). Zürich has high levels of cycling with 15% of its population cycling daily and 20% cycling 2–5 times per week. The number of cycling trips within the city is expected to double by 2025 (Stadtrat Zürich 2012). As of this moment, three bike-sharing systems are in operation in the study area. The largest is the station-based PubliBike which operates a fleet of more than 2000 bicycles (PubliBike AG 2018). The other two companies are Bond and Lime Bikes which have 600 and 500 dockless e-bikes in operation (Neutron Holdings, Inc. 2017; BOND Mobility AG 2020).

Data of bike rides within Zürich was obtained from the bike-sharing company Bond. Bond operates a dockless bike-sharing system of e-bikes. The data contains information on the location and time of origin and destination of each bike ride. A total of 5321 trips are included in the dataset and they cover 22 days from February 1 to 23, 2020. The data was used to evaluate the results of the GIS-MCDA proposed in this study. To define the geofences candidate locations a dataset of publicly accessible bike racks was obtained from the city of Zürich. It comprised 1932 bike and motorcycle parking spaces. A dataset of existing bike-sharing stations run by PubliBike AG was acquired and used to evaluate the geofences proposed in the case study. Data to quantify and model the factors that affect bike-sharing suitability was acquired from different sources. The criteria employed were identified in a literature review in section 2.1. See Table 1 for an overview of the criteria and corresponding datasets.

Table 1. Criteria employed in the Multi-Criteria Decision Analysis. The tag=value pairs classify data in OpenStreetMap.

Criterion	Variable	Data Source (tag=value, for OSM)	Geometry	No. of instances
Public transit large (i.e. train stations) (PTL)	Proximity	OpenStreetMap (railway=station)	Point	27
Public transit small (i.e. tram and bus stops) (PTS)	Proximity	OpenStreetMap (highway=bus_stop, railway=halt, railway=tram_stop, public_transport=station, amenity=bus_station)	Point	1148
Major bike paths (MBP)	Proximity	City of Zürich	Line	1511
Sports facilities and parks (SP)	Proximity	Opendata.swiss	Point and Polygon	682
Higher education (i.e. universities and colleges) (EDU)	Proximity	OpenStreetMap (amenity=university, amenity=college)	Point and Polygon	33
Commercial areas (COM)	Density	OpenStreetMap (office=True, shop=True)	Point	3895
Population (POP)	Density	Opendata.swiss	Raster	-
Entertainment facilities (ET)	Density	OpenStreetMap (amenity=theatre, amenity= cinema, amenity=restaurant)	Point	1084

Wherever possible, data published by governmental organizations was acquired. Where no such data was available, the data was taken from OpenStreetMap (OSM). OSM is an open-source mapping project that is based on the collection of volunteered geographic information by citizens (Goodchild 2007). A dataset representing major bike routes was attained from the city of Zürich. These are specified in the Masterplan Velo which is a policy paper of the city of Zürich that aims to promote bicycle traffic (Stadtrat Zürich 2012). These routes make up the core of the cycling infrastructure in the study area and comprise two types of bicycle paths: (1) routes designed for commuting, high traffic levels, and fast cycling and (2) comfort routes for recreational use which are largely separated from motorized traffic. Two more datasets were retrieved from the city of Zürich, namely cadastral data, and a dataset of sports facilities such as gyms, swimming pools, tennis courts, and similar facilities. From the cadastral data, the locations of parks and green spaces were extracted using the classes assigned by the data distributor. For the criterion population density, a dataset of total resident population per hectare was retrieved from the Swiss Federal Statistical Office for 2019 (Bundesamt für Statistik 2020). All other data for computing the criteria layer was retrieved from OSM via Overpass API (OpenStreetMap contributors 2021). Overpass API is the Application Programming Interface used to query and extract and data from OSM. The query is constructed with tag-value pairs which are used in OSM to classify and describe features (OpenStreetMap Wiki 2020). For the tag-value pairs used to retrieve the datasets for this study refer to Table 1. The criteria for which data was taken from OSM are small and large public transit stations, commercial and office buildings, entertainment facilities (i.e. restaurants, cinemas, and theaters), and university and college buildings and campuses.

3.2 Selection of MCDA method

The MCDA method applied in this study was chosen based on the framework developed by Wątróbski et al. (2019). This framework classifies MCDA methods based on a number of questions that describe the decision problem. The problem of selecting geofence locations, which is the topic of this study, can be described in accordance with the framework as follows:

1. The criteria (i.e. explanatory factors for bike-sharing usage) have varying degrees of influence and can therefore be meaningfully combined using weights.

2. The scale used to describe the criteria performance is quantitative (i.e. proximity and density).

3. It can be assumed that the criteria weights are not influenced by uncertainty as the experts that were consulted for the pair-wise comparison are professionally involved in bicycle traffic planning or bike-sharing. Their expertise thus serves as a strong enough foundation to conduct a certain pair-wise comparison of the criteria.

4. The desired outcome of the MCDA is a ranking of all candidate locations from which the final locations can be selected.

Based on this description of the decision problem and the aforementioned framework it was decided to develop a combined AHP-VIKOR approach in this study. The analytic hierarchy process (AHP) was utilized to determine criteria weights and VIKOR (VlseKriterijumska Optimizacija I Kompromisno Resenje; i.e. multi-criteria optimization and compromise solution) was used to aggregate the criteria and rank the alternatives. VIKOR originates in compromise programming and compares the closeness of the alternatives to the ideal and negative-ideal solution (Opricovic and Tzeng 2004).

3.3 Analytic hierarchy process

Based on the criteria that were found in the literature review, an AHP was conducted to assess the level of influence of the individual criteria and to quantify this as priority weights that can be used in the GIS-MCDA. A similar approach was used by Kabak et al. (2018) for station-based bike-sharing. Malczewski (2006) found that 9.6% of more than 300 GIS-MCDA related articles published between 1990 and 2004 used AHP. This shows that the method is well established and used in GIS-MCDA. In infrastructure management and planning, AHP is the most common MCDA method with growing usage (Kabir et al. 2014). Here, the main field of application is transportation infrastructure. AHP is particularly useful as it can structure the partly strongly diverging views of different stakeholders (Ramanathan 2001).

The AHP was proposed by Saaty (1980) as a method for structuring decision problems in social, economic, and management sciences. The method consists of four steps: (1) the structuring of the decision problem, (2) pair-wise comparison, (3) calculation of weights and consistency of the pair-wise comparison, and (4) the aggregation of local weights for each alternative.

In the case of this study, the decision problem (1) is where to place geofences for dockless bike-sharing. The problem was structured (2) by finding criteria that affect bike-sharing usage in the relevant literature (Table 1).

For the pair-wise comparison of these criteria (3) the expertise of people that are involved in bike-sharing companies and the planning of cycling infrastructure was sought. Around 5 to 10 participants are regarded as sufficient to gain consistent weights in AHP if they are experts in the topic of the decision problem (Cheng and Li 2001; Daim et al. 2013; Sanchez-Lozano et al. 2016). It is furthermore advisable to include experts with different backgrounds to obtain a holistic overview of

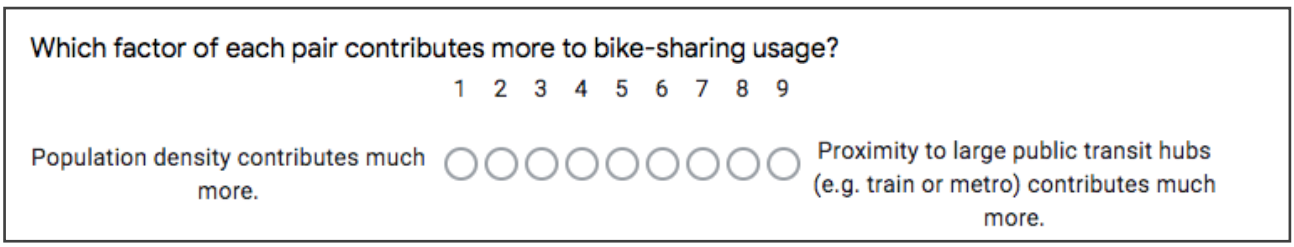

Figure 3. Example of question from the analytic hierarchical process survey.

the decision problem (Sirikrai and Tang 2006). Potential experts for this study were identified by studying the bike-sharing market, relevant municipal and research activity related to bike-sharing, and micro-mobility in Zürich. To ensure that the experts had good knowledge of the study area only people that were based or active in Zürich were approached.

The experts were asked to fill out a survey and to give a ranking for each pair of criteria (Figure 3). Additionally, before the survey was sent to the experts, one of them was asked to provide feedback on the criteria suggested for the survey. Using their feedback, the criterion public transit was split into two criteria, one for small and large stations respectively. The ranking ranged from 1 to 9 where 1 meant that the left criterion contributes more to bike-sharing usage. While a value of 9 meant that the right criterion contributes more to bike-sharing usage. The center value 5 in contrast meant that both criteria contribute equally to bike-sharing usage. This ranking scale varies from the standard intensity scale used in AHP, ranging from 9 to 1 and from 1 to 9. It was decided to use a simpler and shorter scale for the survey to make it easier for the respondent to answer the survey. This was decided because of the large number of 8 criteria which made the comparison complex. A simpler ranking scale reduced the amount of information shown in the survey and made the ranking faster. Before compiling the rankings into a pair-wise comparison matrix they were transformed into the scale used in the AHP (see Table 2).

Table 2. Conversion of ranking weights used in the survey to intensity weights used in AHP.

Survey ranking	AHP intensity weights	Definition
1	1/9	Criterion i contributes extremely less than criterion j.
2	1/7	Criterion i contributes very strongly less than criterion j.
3	1/5	Criterion i contributes strongly less than criterion j.
4	1/3	Criterion i contributes moderately less than criterion j.
5	1	Both criteria contribute equally.
6	3	Criterion i contributes moderately more than criterion j.
7	5	Criterion i contributes strongly more than criterion j.
8	7	Criterion i contributes very strongly more than criterion j.
9	9	Criterion i contributes extremely more than criterion j.

As proposed by Aczél and Saaty (1983), the pair-wise comparison weights assigned by the various experts were aggregated by computing the geometric mean (Equation 1). The geometric mean must be used here as the resulting pair-wise comparison matrix must be reciprocal and other aggregation methods such as the arithmetic mean would not preserve this property.

$$\left(\prod_{i=1}^{n} x_i\right)^{\frac{1}{n}} = \sqrt[n]{x_1 x_2 \cdots x_n} \tag{1}$$

Where x_i is the value given for the current pairwise comparison by the i-th respondent. The means were entered in n times n pair-wise comparison matrix A (Equation 2).

$$\mathbf{A} = (w_i/w_j)_{n\times n} = \begin{pmatrix} w_1/w_1 & w_1/w_2 & \dots & w_1/w_n \\ w_2/w_1 & w_2/w_2 & \dots & w_2/w_n \\ \vdots & \vdots & \ddots & \vdots \\ w_n/w_1 & w_n/w_2 & \dots & w_n/w_n \end{pmatrix} \tag{2}$$

Where w_i and w_j are the intensity weights of each pair-wise comparison. This can be simplified and rewritten as (Equation 3, Brunelli 2015):

$$\mathbf{A} = \begin{pmatrix} 1 & a_{12} & \cdots & a_{1n} \\ \frac{1}{a_{12}} & 1 & \cdots & a_{2n} \\ \vdots & \vdots & \ddots & \vdots \\ \frac{1}{a_{1n}} & \frac{1}{a_{2n}} & \cdots & 1 \end{pmatrix} \tag{3}$$

Where a_{1n} is the weight assigned to criterion 1 when comparing it to criterion *n* and $1/a_{1n}$ is the weight of criterion *n* when comparing it to criterion 1 which is the reciprocal of a_{1n}.

In the next step, the pair-wise intensity weights were aggregated by obtaining the normalized eigenvector of the comparison matrix. This vector is called priority vector and contains weights that sum up to 1. These weights were used for the following parts of the GIS-MCDA. Additionally, the consistency of the comparison matrix was tested by computing the consistency index CI (Equation 4; Saaty, 1980):

$$CI(\mathbf{A}) = \frac{\lambda_{\max} - n}{n-1}. \tag{4}$$

Where λ_{max} is the maximum eigenvalue of matrix *A*. This was rescaled to receive the more meaningful consistency ratio CR (Equation 5; Saaty, 1980).

$$CR(\mathbf{A}) = \frac{CI(\mathbf{A})}{RI_n} \tag{5}$$

Where RI_n is the random index that depends on the number of criteria employed in the AHP. For the 8 criteria included in this study, the random index is 1.4057 (Alonso and Lamata 2006). The *CR* can be interpreted as the following: A *CR* of 0.2 would mean that the weights are 20% as inconsistent as randomly generated weights . In practice, a CR of ≤ 0.1 should be aimed for (Saaty 1980).

3.4 Creation of criteria layers

Several raster layers had to be computed to get data that represented the criteria considered in this study. These raster layers will be referred to as criteria layers. For the calculation of the various criteria layer two algorithms were developed and implemented. For this the programming language Python was used (Van Rossum and Drake 2009). Two measures were computed, namely proximity and density. This was decided since cycling levels are affected in different ways by the criteria. For some criteria, the distance to the nearest instance is of relevance (e.g. for public transit) whereas for other criteria it is rather the overall density at a location that contributes to bicycle usage (e.g. density of shops, restaurants). The data that was used to compute the criteria layers was acquired from OSM, the city of Zürich, and the Swiss Statistical Office (see Section 3.1).

3.4.1 Proximity layers

For the proximity calculation for the various criteria locations, a target raster covering the study area with a spatial resolution of 50 m was created. This resolution was chosen as a compromise between detail and processing time. It was assumed that the suitability would not significantly change over this small distance. Areas outside the boundary of the city were masked out. Only cells that had an overlap with a buffer of 10 m along the bike network were processed in further analysis. This was decided as the geofence location should be along a road or bike path. Cells that are not close to any road were therefore not relevant for further analysis. Excluding these cells also decreased the processing time of the algorithm. The proximity was calculated in network distance to get a meaningful metric. For this, a network graph was created from OSM data using the OSMnx Python module (Boeing 2017). Streets and bike paths that were classified as being bikeable were retrieved and used to construct the network graph.

The algorithm computed the shortest path from each cell center in the target raster to the nearest instance of each criterion. For polygon layers (e.g. parks and university campuses) the distance to the centroid was computed. For the bike paths, the distance to the closest line segment was computed. To decrease computational complexity a heuristic was implemented in the distance computation. It was used to find the instances with the shortest Euclidean distance. The more demanding network distance computation was only conducted for these closest instances. The network distance computation utilized Dijkstra's algorithm. The subset of instances for which the network distance was computed included the 4 closest facilities of each cell. This number was chosen after running a sensitivity analysis for different values of this parameter (Figure 4).

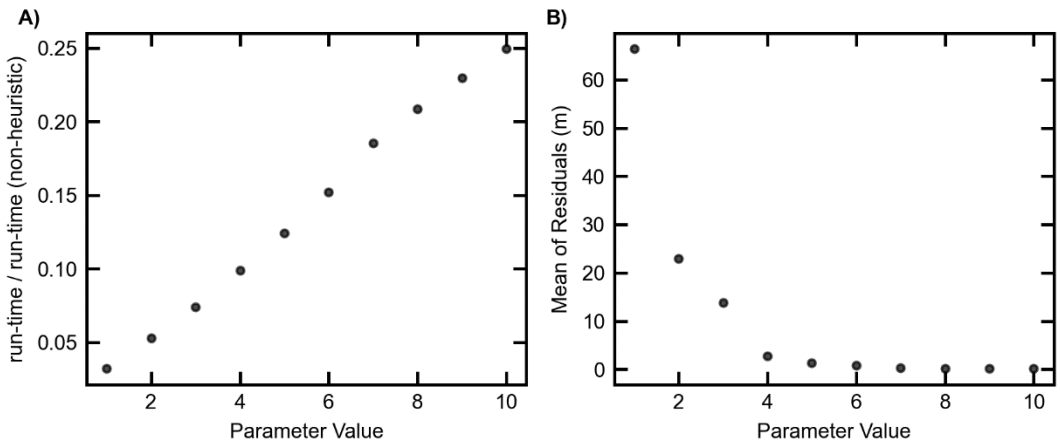

Figure 4. The results of the sensitivity analysis used to determine the value for the proximity heuristic's parameter. The ratio between the run-time of the algorithm using the heuristic and the run-time of the non-heuristic algorithm as a function of the parameter is shown to the left (A). The mean of the residuals of the output of the heuristics is shown to the right as a function of the parameter (B). The parameter specifies for how many instances the network distance is computed.

For the sensitivity analysis the proximity to facilities of higher education was computed with different parameter settings. The parameter ranged from 1 to 10 and the resolution was set to 100 m. The parameter range specifies the number of closest instances in Euclidean distance for which the network distance was computed. The proximity layer was also computed without the heuristic, solely by network distance. This was used as the ground truth data to evaluate the outputs created with the various parameter settings. The criterion EDU was chosen as it featured the smallest number of instances, namely 33 (Table 1). Comparing the ground truth with the outputs of the different parameter settings showed that a value of 4 gave a reduction in processing time of about 90% while returning an output similar to the ground truth. The mean residual of the proximity was smaller than 2.6 m. This was assumed to be an acceptable deviation from the ground truth.

3.4.2 Density layers

The criteria COM and ET considered the density of instances. This was computed like the proximity layers with a target raster of 50 m spatial resolution. For each cell in this raster, a neighborhood analysis was performed in which all instances (e.g. restaurants, theaters, shops, or office buildings) that overlapped a 2 km buffer around the cell center were registered. The count of these instances was stored in the respective target raster cell.

The size of the neighborhood buffer was derived from three different studies that found that up to 90% of the bike-trips in dockless and station-based bike-sharing are shorter than 2 km (Liu et al. 2018; Dong et al. 2019; Ma et al. 2020). Based on this it can be assumed that criteria facilities outside of the 2 km buffer are not of high relevance for the suitability of a location as most of the bike trips will not reach them. Thus they will not significantly contribute to the bike-sharing levels of the location.

3.4.3 Standardization

The criteria layers were standardized by applying Keeney's value function (Keeney 1992). The value function is a mathematical representation of the desirability of a criterion value. By applying a value function the criteria values were standardized to the range 0 for least desirable to 1 for most desirable criteria values. Standardizing the criteria layer makes it possible to compare their suitability values. In this the standardized layers were used to create the Weighted Linear Combination and to create maps for visual comparison of the criteria performance within the study area. Equation 6 was used for criteria that should be minimized, that is where a small criteria score is desirable.

$$v(a_{ik}) = \left(\frac{max\{a_k\} - a_{ik}}{max\{a_k\} - min\{a_k\}} \right)^{\rho} \quad (6)$$

where k is the criterion, $v(a_{ik})$ is the standardized value and a_{ik} is the value of the criterion. The variables $max\{a_k\}$ and $min\{a_k\}$ are the maximum and minimum values for the criterion respectively. ρ is a parameter that is defined by the decision-maker and can be interpreted as reflecting the risk affinity of the decision-maker. In this study, ρ was set to 1 which results in a linear standardization. For those criteria that should be maximized, meaning where a high criteria score is desirable, equation 7 was used.

$$v(a_{ik}) = \left(\frac{min\{a_k\} - a_{ik}}{max\{a_k\} - min\{a_k\}} \right)^{\rho} \quad (7)$$

In this study, layers representing proximity were standardized using equation 6, meaning that close distance is regarded as being more desirable. Layers that contained density values were maximized, as related research has found a relationship of higher density of population and entertainment facilities to be linked to higher bike-sharing usage (e.g. Li et al., 2020; Wang et al., 2018).

3.5 Weighted linear combination

The criteria layers were combined using a weighted linear combination (WLC) which is one of the most common algorithms for GIS-MCDA. The core operation of the algorithm is intuitive to understand and is described by equation 8 (Pereira and Duckstein 1993; Jiang and Eastman 2000):

$$V(A_i) = \sum_{k=1}^{n} w_k v(a_{ik}) \quad (8)$$

where $V(Ai)$ is the combined suitability value, w_k is the weight, and $v(a_{ik})$ is the value function for the criterion. If the data that is used is in a raster format, implementing this method in an algorithm is straightforward and can be done by using map algebra. The raster layers comprising the standardized values are multiplied with the corresponding weights that were determined in the AHP. The resulting

layers are then added to each other which results in a suitability map. The suitability map created by WLC was not used for the geofence selection itself. It served mainly the visualization of spatial variation in suitability. If a bike-sharing system was launched with initial geofence locations as proposed by this GIS-MCDA framework the suitability map can be used to identify possible gaps in the geofence network. It can also be used to find suitable locations for additional geofences if the network should be extended.

3.6 Candidate locations

For a location selection framework candidate locations from which to select the final sites are necessary. The placement of these can be challenging, particularly in the urban space where relatively limited space is being used by many different actors and for many different purposes. Previous planning of bike-sharing stations and geofences has either placed potential locations with an even spacing along a road network, utilized cluster analysis and bike-trip data or manually selected potential locations (Conrow et al. 2018; Kabak et al. 2018; Zhang et al. 2019). The latter is only feasible for a small area or if only few stations are to be added to an existing network. The framework developed in this study is designed to function even in cities where no bike-trip data is available. Hence, the clustering approach could not be adapted. Placing evenly spaced candidate locations along a road network does not consider the complexity of urban space and will likely result in candidates at places that are not suitable for a geofence; either due to space limitations or usage restrictions.

Instead, it was decided to use already existing infrastructure for bike parking. García-Palomares et al. (2012) used a similar approach for bike-sharing station planning. They placed candidate locations at every public transit station that exceeded a threshold of daily commuters. For the case study, a dataset of bike parking spots was acquired and used as a source for candidate locations. Using bike parking spots as candidates ensures that space for parking bikes is available at every potential location and encourages the user to park the shared bike properly. From this dataset, only the 1309 bike parking spots that had space for 10 or more bikes were taken into consideration. Parking spots that were exclusively designated for motorcycles were also excluded from further processes. If this framework was to be applied to a city for which no dataset of bike parking is available this data could be obtained from OSM.

3.7 Location selection

The selection of locations for the geofences was done by taking the spatial distribution of the candidate locations relative to each other and their suitability into consideration. This was realized in a novel discrete location selection model that applied a suitability ranking of the alternatives and a variable minimum distance constraint between the candidate locations (García-Palomares et al. 2012). The suitability ranking was computed using VIKOR. VIKOR was developed for multi-criteria analysis of complex systems by Opricovic and Tzeng (2004). It expresses the suitability of an

alternative in terms of its closeness to the ideal solution. In this study, VIKOR will be adopted to rank the candidate locations based on their closeness to the ideal solution.

First, the candidate locations were ranked using VIKOR, then they were iteratively added to the final set of geofences. This was initialized by adding the highest-ranking candidate location to the geofence selection. Next, the second-highest-ranking candidate location was evaluated by checking its distance to the previously added location. If the distance exceeded a minimum distance, the current candidate location was added to the final set. This was repeated for all other candidate locations by checking the distance to all geofences previously added to the final geofence set. The minimum spacing constraint is based on studies by Fuller et al. (2011) and Tran et al. (2015) who found a spacing of 200 to 500 m between bike-sharing facilities suitable for optimizing usability and increasing usage of bike-sharing systems. Wang et al. (2018) also defined the service area of a bike-sharing station as a 500 m radius. The spacing constraint was defined as a function of suitability. For the most suitable candidate locations, a distance constraint of 200 m was used. For the least suitable candidates, this constraint was set to 500 m. The thresholds for the most and least suitable candidate locations were defined as the 10% and 90% percentile of the VIKOR ranking. For suitability values between these thresholds, the spacing constraint was determined by a linear relationship that was assumed (Figure 5). The least suitable candidates were regarded as being unsuitable and excluded from the selection process as they were entirely located at the outskirts of the study area. This decision was based on the visual inspection of the spatial distribution of these locations (Section 4.3).

3.8 VIKOR

The VIKOR ranking was implemented in Python using the modules Numpy, Geopandas and Rasterio (Gillies 2019; Harris et al. 2020; Jordahl et al. 2021). The criteria values at the candidate locations were retrieved from each criteria layer. This was done by taking the value of the cell in which a candidate location was sited. The VIKOR ranking can be divided into a 4 step process.

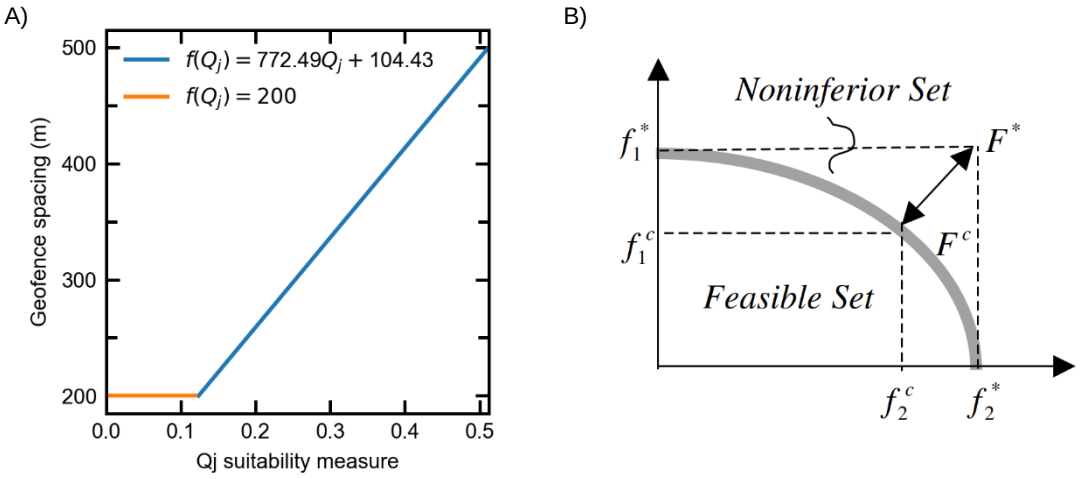

Figure 5. Linear functions used to compute the minimum spacing between geofence locations (A). Illustration of compromise solutions in comparison to ideal solution (B). Source: Opricovic and Tzeng, 2004

(1) The first step was to find the best (f_i^*) and worst (f_i^-) score among the candidate locations for each criterion. For criteria that should be minimized the best score is equal to the lowest criteria value and the worst score is the highest one. The opposite applies to criteria that should be maximized. Figure 5 shows the relationship between the ideal solution $F^*$and compromise solutions F^c which would result from choosing any of the alternatives.

(2) Next the measures S_j and R_j were computed for each candidate location. These measures are the weighted normalized Manhattan distance L_1 and the weighted normalized Chebyshev distance L_∞ respectively. They are used as boundary measures for the ranking of alternatives in VIKOR. S_j can be interpreted as the distance in criteria space of the j-th alternative to the ideal solution and is computed according to equation 9.

$$S_j = \sum_{i=1}^{n} \frac{w_i(f_i^* - f_{ij})}{f_i^* - f_i^-} \tag{9}$$

where x_{ij} is the criteria score of the i-th criterion and the j-th alternative, and w_i is the i-th criterion's weight that was determined in the AHP. Selecting the alternative with the smallest S_j as a solution would mean to maximize group utility. R_j was computed by equation 10 which returns the largest summand of equation 9. This can be interpreted as the closeness of the worst performing criterion for the j-th alternative to the ideal solutions criteria score for this criterion.

$$R_j = \max_j \left[\frac{w_i(f_i^* - f_{ij})}{f_i^* - f_i^-} \right] \tag{10}$$

(3) Next the measure Q_j which aims to balance S_j and R_j was calculated for each candidate location (Equation 11).

$$Q_j = v\frac{(S_j - S^*)}{(S^- - S^*)} + (1 - v)\frac{(R_j - R^*)}{(R^- - R^*)} \tag{11}$$

where the weight v is set according to a strategy of maximum group utility. A value of 0.5 represents a consensus driven strategy and is commonly used in VIKOR. S^*, S^-, R^*, R^- are the minimum and maximum values of S_j and R_j among all alternatives:

$$S^* = \min_j S_j,$$
$$S^- = \max_j S_j,$$
$$R^* = \max_j R_j,$$
$$R^- = \max_j R_j,$$

(4) The last step in the VIKOR procedure was to order the candidate locations according to their Q_j ranking. As Q_j is a measure of closeness to the ideal solution a small value is favored.

3.9 Assessment of geofence locations

To assess the proposed geofence locations the actual bike-sharing demand will be computed from the bike-usage data acquired from BOND Mobility AG. Demand studies are commonly conducted by aggregating departures and arrivals on a zonal level. The zones used for the aggregation of usage data can have different shapes and can greatly affect the resulting bicycle usage maps (Shui and Szeto 2020). Zhang et al. (2019) superimposed a uniform grid over their study area and counted departures and arrivals for each grid cell. Such a grid-based approach has been criticized for its simplification of the complex urban environment (Dong et al. 2019). Frade and Ribeiro (2015) studied the demand for the optimization of bike-station locations and used administrative boundaries to aggregate bicycle usage data.

In this study, the demand covered by the geofences will be evaluated on the geofence-level by computing the number of bike trip origins and destinations (OD) within a 500 m buffer around each geofence. This buffer size is based on Frade and Ribeiro (2015) who recommend that no two points in a demand zone should be more than 500 m apart from each other and Wang et al. (2018) who define the service area of bike-sharing stations as a 500 m radius. Additionally, a network distance analysis was conducted that computed the proportion of ODs that were within 500 m network distance of a geofences. This aimed to test the extent to which the demand for bike-sharing is covered by the proposed geofences. To assess the general accessibility of the geofence locations the average network distance from any point within the street network of the study area was computed.

Furthermore, the proposed geofence locations were compared to the existing bike-sharing stations in the study area. The bike-sharing stations served as a ground truth data set in this context. The OD count per station 500 m buffer, the proportion of ODs within 500 m network distance to a station and the average network distance to stations was also computed for the stations. This allowed to assess how well the geofence locations performed compared to an existing bike-sharing parking system. The OD count was used to evaluate the extent to which the suitability value Q_j related to actual bike-sharing usage. For this the OD count was plotted against the Q_j value.

3.10 Geofence capacity

There exists previous research on the capacity planning of bike-sharing stations (e.g. García-Palomares et al. 2012). Zhang et al. (2019) and Cheng et al. (2019) showed that this concept can be transferred to geofence capacity determination. However, these approaches base the calculation on demand estimates that are based on bike-trip data. Since the aim of this study is to develop a framework that can be applied to a city for which such data is not available, a different approach had

to be adopted. Instead of using the demand data directly, it was decided to use the suitability ranking as a proxy for demand and to derive the geofence capacity from the suitability.

According to Zhang et al. (2019) and García-Palomares et al. (2012), in practice it is common to select a fixed number of bikes for each geofence for instance 10 or 20. This range will be used in this study too. However, the approach that was developed for this study uses existing bike parking infrastructure. In order to avoid conflict with regular bike users it was decided to include the available number of bike racks at the geofence locations in the capacity determination. The maximum number of shared bikes parked at a geofence was limited to 50% of the bike racks available at a location. This was decided since bike-sharing should not compete with normal bike users who also seek bike parking. Only bike parking spots with at least 10 bike racks were considered as candidate locations. Hence, the smallest possible geofence capacity is 5. The capacity was computed based on the available bike racks and the suitability ranking and followed the scheme shown in Table 3. The class boundaries for the Q_j value were defined by the 25%, 50% and 75% percentiles.

Most approaches to bike-sharing station and geofence capacity known to the author take the fleet size into account to evaluate the computed capacities (García-Palomares et al. 2012; Cheng et al. 2019; Zhang et al. 2019). The companies that operate dockless bike-sharing in Zürich, Bond Mobility and Lime Bikes have fleet sizes of 600 and 500 bikes, respectively. Since the bike ride data that will be used for the assessment of the result was acquired from BOND Mobility AG a fleet size of 600 bikes was assumed. The capacity was furthermore evaluated by dividing the OD data into 1 hour intervals. A neighborhood analysis was performed for each of the ODs that occurred in an interval. This analysis involved counting the ODs and summing up the capacity of all geofences within a 500 m radius. The number of ODs was subtracted from the available capacity to test whether the capacity was sufficient for the place and time.

Table 3. Conversion scheme for Qj suitability measure to maximum geofence capacity. The class boundaries for the Qj classification were derived from the 25, 50 and 75% percentiles. The Qj range is valid for the case study. The geofence capacity was constrained by the available parking spots at a geofence location.

Percentiles defining boundaries	**Qj suitability range**	**Maximum Geofence Capacity**
- 25%	< 0.16	20
25% - 50%	0.16 - 0.24	15
50% - 75%	0.24 - 0.37	12
75% -	> 0.37	10

4 Results

The explanatory criteria that were used in the AHP and VIKOR were identified in the literature review in section 2.1 and are compiled in Table 1. The other results are presented in the following sections.

4.1 Analytic hierarchy process

The AHP results are based on the response from 5 experts. Of those experts, two came from the bike-sharing industry, one was active in related research, one worked at the municipal traffic planning administration and one for an non-governmental organization working to promote cycling.

The pair-wise comparison matrix that was aggregated from the expert ranking is shown in Table 4. The criteria EDU and PTL were found to contribute more to bike-sharing usage than the other criteria. They mostly received higher intensity weights than the other criteria. This is also underlined by the normalized priority vector weights which show the overall influence of the criteria. These weights were used for the geofence location selection. The most influential criteria EDU and PTL received priority weights of 0.23 and 0.21, respectively. They are followed by the criteria ET, COM, POP, and SP which feature weights ranging from 0.10 to 0.14. The criteria that received the lowest weights are PTS and MBP, the latter got the marginal weight of 0.04. The consistency analysis showed that the comparison matrix is consistent with a consistency ratio of 0.017. This expresses that the rankings are 1.7 % as inconsistent as if they were made randomly. According to Saaty (1980), a consistency ratio of smaller 0.1 can be accepted. Hence, the results of the AHP conducted in this study can be used for the GIS-MCDA.

Table 4. Pair-wise comparison matrix with intensity weights aggregated from the expert ranking. The priority weights are shown in the right-most column.

	MBP	**PTL**	**PTS**	**EDU**	**SP**	**COM**	**POP**	**ET**	**Priority weights**
Major Bike paths (MBP)	1.00	0.23	0.68	0.22	0.34	0.30	0.32	0.25	**0.04**
Public Transit large (PTL)	4.36	1.00	3.16	0.80	2.37	1.90	1.53	2.29	**0.20**
Public Transit small (PTS)	1.48	0.32	1.00	0.40	0.53	0.52	0.64	0.35	**0.06**
Higher education (EDU)	4.58	1.25	2.54	1.00	3.32	2.54	1.93	1.72	**0.23**
Sports facilities and parks (SP)	2.95	0.42	1.904	0.30	1.00	0.80	1.64	0.58	**0.10**
Commercial areas (COM)	3.32	0.53	1.93	0.39	1.25	1.00	0.95	1.00	**0.11**
Population density (POP)	3.16	0.65	1.55	0.52	0.61	1.05	1.00	0.73	**0.11**
Entertainment (ET)	4.08	0.44	2.85	0.58	1.72	1.00	1.38	1.00	**0.14**

4.2 Criteria layers

The standardized criteria layers show a clear spatial distribution of high and low suitability for bike-sharing. Figure 7 shows the standardized criteria layer which can be used to compare spatial differences in suitability among the criteria. All criteria indicate higher suitability for bike-sharing towards the city center which is located north of the lake. This is most prominent for the criteria COM and ET. They have very high suitability exclusively in the city center and a quickly decreasing suitability toward the suburbs. Other criteria such as MBP and PTS stations have mostly high suitability in large parts of the study area. The remaining three criteria layers for PTL, SP, and EDU exhibit high suitability for most parts of the study area except for some patches of low suitability mostly at the edge of the city. The overall suitability that is shown in the weighted linear combination reflects similar patterns as the criteria layer (Figure 6a). The results indicate that high suitability can also be expected in sub-centers in the north and northwest of Zürich. Most areas on the outskirts of the study area received rather low suitability values with the lowest being at the southeasternmost boundary. This area is mostly forest and not characterized by urban structures.

4.3 VIKOR ranking

VIKOR was used to rank the candidate locations according to their closeness to the ideal solution. Figure 8 shows the statistical distribution of the Qj measure that was used for the ranking. As Qj represents the closeness to the ideal solution, smaller values are more suitable. The distribution is left-skewed with a mean of 0.3 and a median of 0.26. The minimum and maximum values are 0.03 and 0.89 respectively. The 10% and 90% percentiles used for computing the spacing constraint (Figure 5) are 0.12 and 0.51, respectively. Most of the highly suitable candidates of a Qj smaller than the 10% percentile were in a commercial area close to the central train station and close to the main university campus. The 90% percentile was used as a threshold to filter unsuitable stations. This resulted in 120 candidate locations being excluded from the selection process. The majority of these candidates were in the outskirts of the study area, in the South, North-West and South-East. Furthermore, there are several candidate locations that were located outside of the criteria layers. They were in cells of the criteria layer that featured no data due to being outside of the bike network buffer (Section 3.4). This was the case for 114 candidate locations. These candidates were also excluded from the further selection process.

To test how well the suitability ranking related to actual bike-sharing demand, the number of ODs in a 500 m buffer around each candidate location was computed. This count was plotted as a function of the Qj suitability measure (Figure 8a). The plot supports the assumption that a relationship between a geofences Qj value and the frequency of bike trips in its vicinity exists. OD frequencies range from 0 to 942 per geofence. Qj values of larger than the 90% percentile of 0.51 have low OD counts with a mean of 49, whereas the overall mean is 281. The relationship between OD count and Qj was furthermore tested by computing Spearman's correlation coefficient. Other statistics such as linear regression and Pearson's correlation coefficient were disregarded since the assumptions of linear

relationship and normality of variables residuals distribution were not satisfied. A Spearman coefficient of -0.81 was computed which indicates a high negative correlation. The correlation was significant with a p-value smaller 0.001.

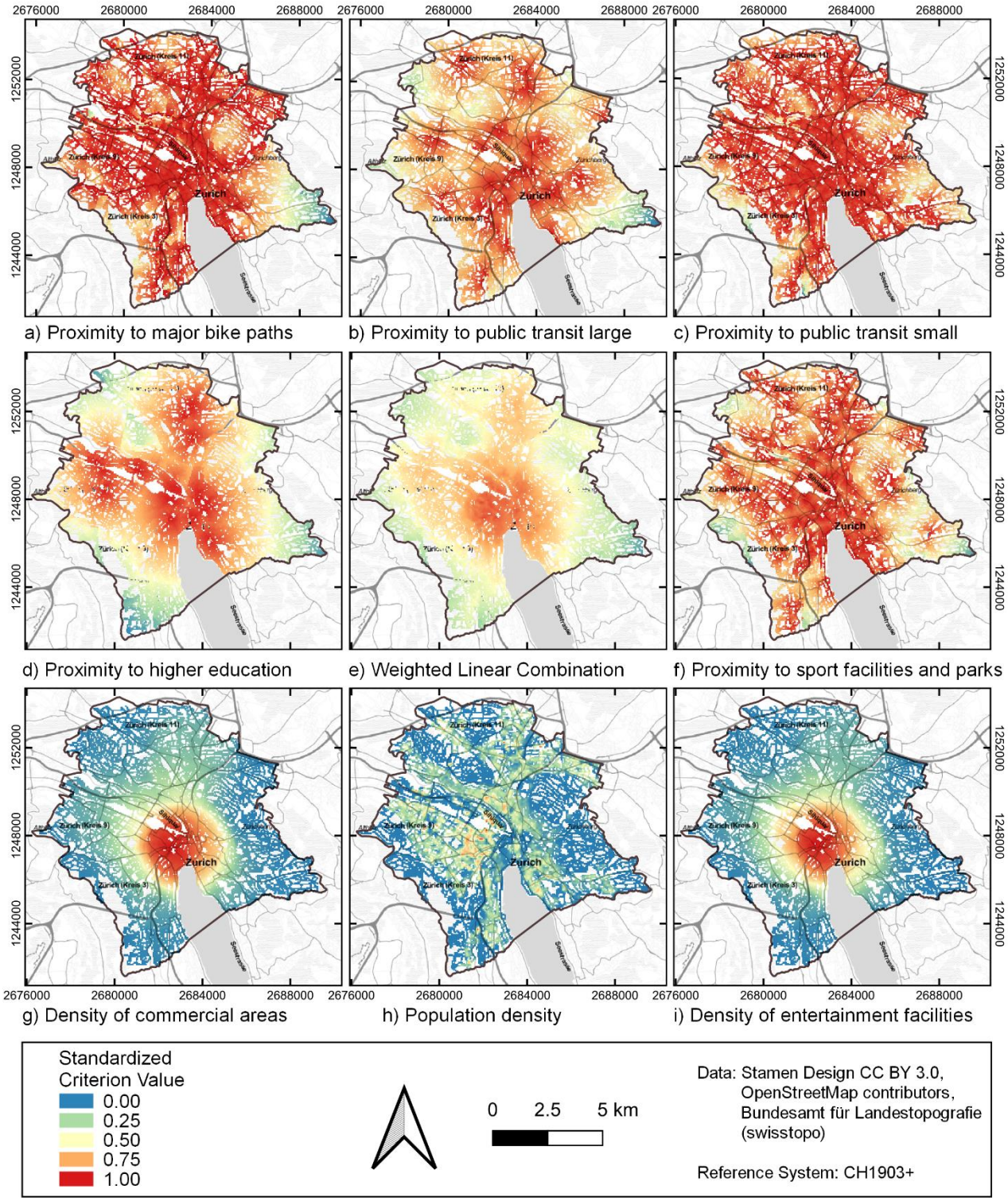

Figure 6. Maps of standardized criteria values with 1 representing high and 0 representing low criteria scores. Map e) shows the linear weighted combination that is a combination of all standardized criteria layers. It can be interpreted as the overall suitability of a location.

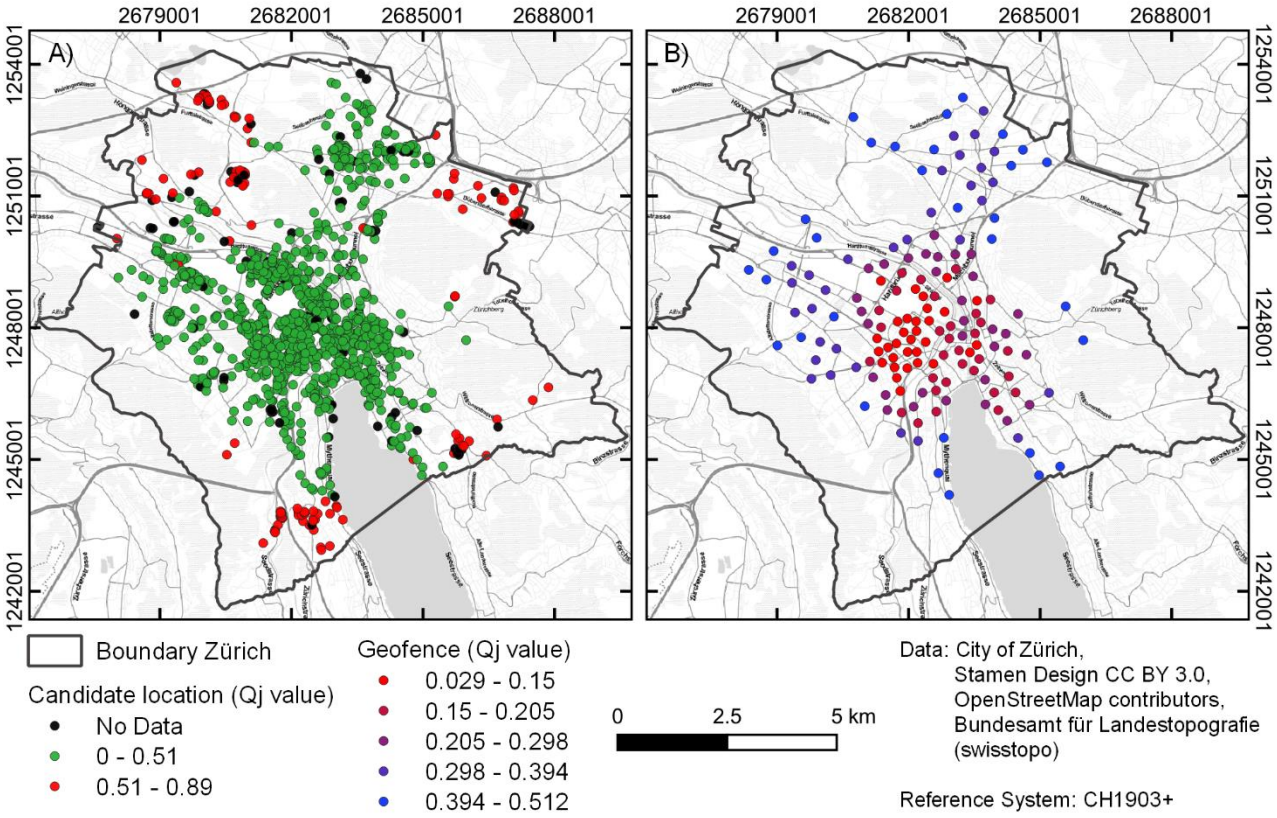

Figure 7. Maps of candidate locations (A) and of selected geofence locations (B). The candidates are categorized into 3 classes. Those with no data, that is those that were located outside of the criteria layers, those with a Qj value of higher than the threshold of 0.51. The locations selected for a geofence are colored according to their suitability ranking. A low Q_j value represents high suitability.

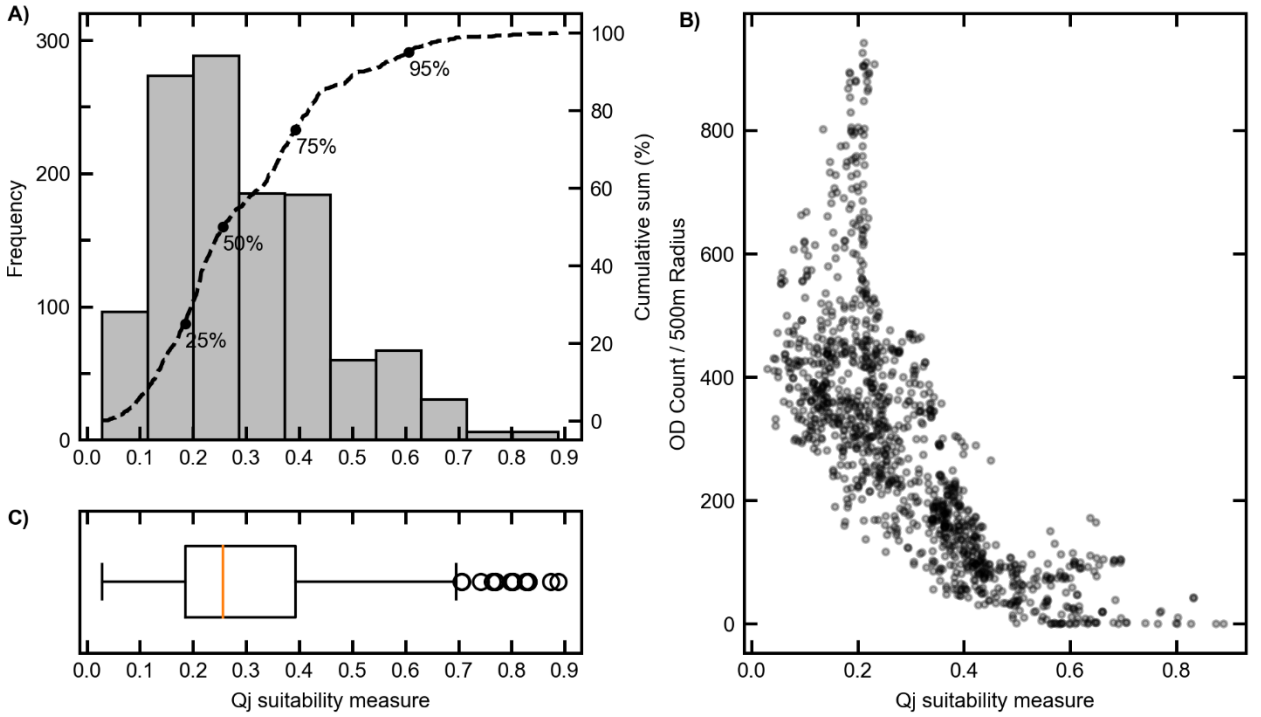

Figure 8. Distribution of VIKOR ranking of the Q_j-measure of closeness to the ideal solution for the geofence candidate locations. A low Q_j value represents a high suitability (A and C). Number of ODs in the 500 m buffer around the geofence as a function of the O_i suitability measure (B).

4.4 Assessment of geofence locations

The location selection resulted in 155 geofence locations (Figure 8b). The geofences have a minimum Q_j suitability value of 0.03 and a maximum of 0.51. The mean is 0.26 and the median 0.24. Figure 9 presents the statistical distribution of the Qj value for the selected geofences. It exhibits a broad distribution of Qj values from close to zero to 0.5 with a mean at 0.26. Furthermore, Figure 9a and 9c show the statistical distribution of the shortest distance to a geofence from the ODs. This distance analysis showed that 81% of the ODs were within 500 m of at least one geofence. Only 5.6% of the ODs were further than 1000 m from any geofence proposed by the location selection framework.

Table 5. Descriptive statistics to compare how well the geofences developed in this study and the existing stations cover the demand for bike-sharing in the study area.

	Count	**Distance OD-to-nearest-station/geofence (m)**		**ODs within <500 m of station/geofence**			**Distance from any point in road network to nearest station/geofence (m)**	
		Mean	Std. Dev	Median	Std. Dev.	Total (%)	Mean	Std. Dev.
Geofences	155	341	311	262	347	81	1395	1051
Stations	170	374	340	269	361	77	1692	1076

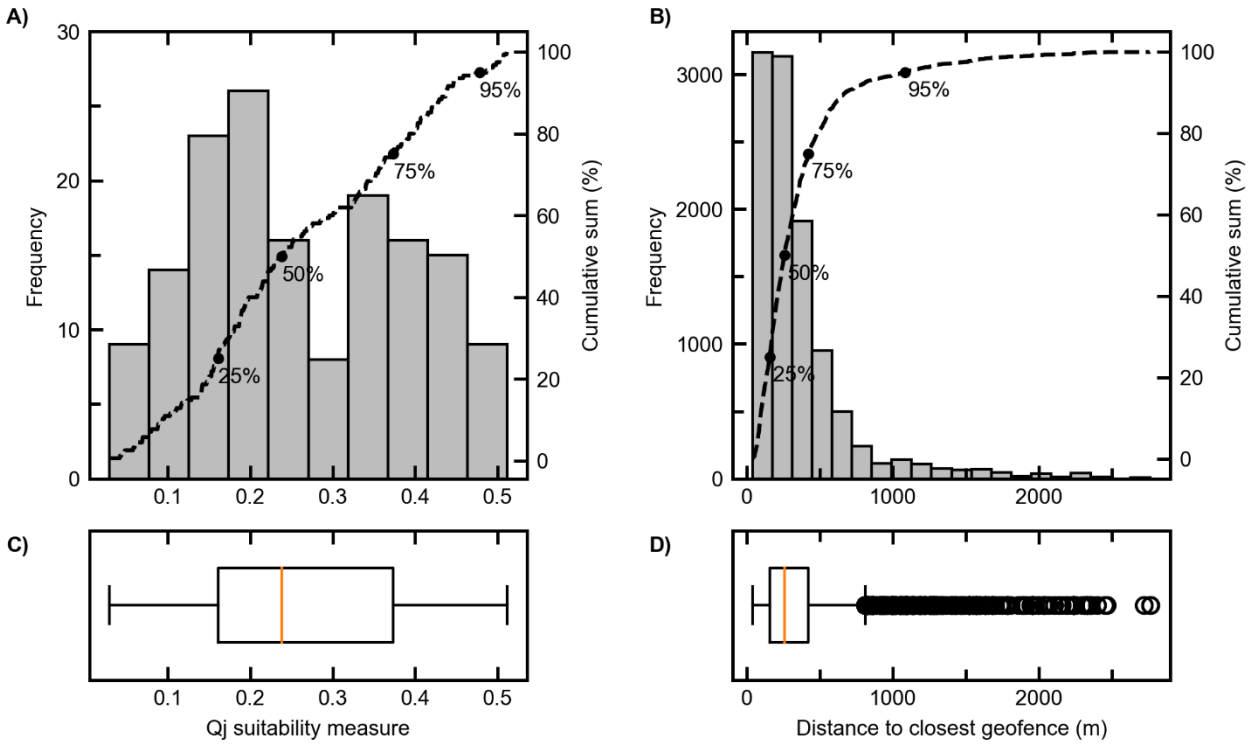

Figure 9. Histogram and boxplot of statistical distribution of the Q_j suitability measure for the selected geofence locations (A and C). Histogram and boxplot of the network distance to the closest geofence from start and end-points of bike trips in the study area (B and D).

The proposed geofences were also compared to bike-sharing stations that existed in the study area. They were compared in terms of accessibility and coverage of ODs (Table 5). The geofences had slightly smaller distances to the ODs with 341 m compared to 374 m for the station network. The station network also had slightly fewer ODs within 500 m network distance to a location. The mean shortest path distance from any point in the road network to a geofence is also shorter than the equivalent of the stations. The geofences have on average less ODs in their proximity but cover a slightly larger proportion of the total count which can be seen on the percentage of ODs that was within a 500 m buffer of any geofence or station.

4.5 Geofence capacity

The frequencies of the various geofence capacities, ranging from 5 to 20 are shown in Figure 9. The proposed geofences have a mean capacity of 8.5 bicycles. More than 75% of all geofences received a capacity of 10 bikes or less. Figure 9 shows that geofences with a capacity of less than 10 bikes are evenly distributed over the study area. They are even frequent in central areas that exhibit comparably high suitability according to the Q_j ranking. Geofences of high capacity between 13 and 20 are more frequent in the areas of high suitability. In the outskirts there are mostly low capacity geofences with capacities of 6 to 8 bicycles. All geofences combined offer a capacity of 1322 bikes. This gives a ratio of 2.2 parking spots at geofences per bike if a fleet size of 600 is assumed.

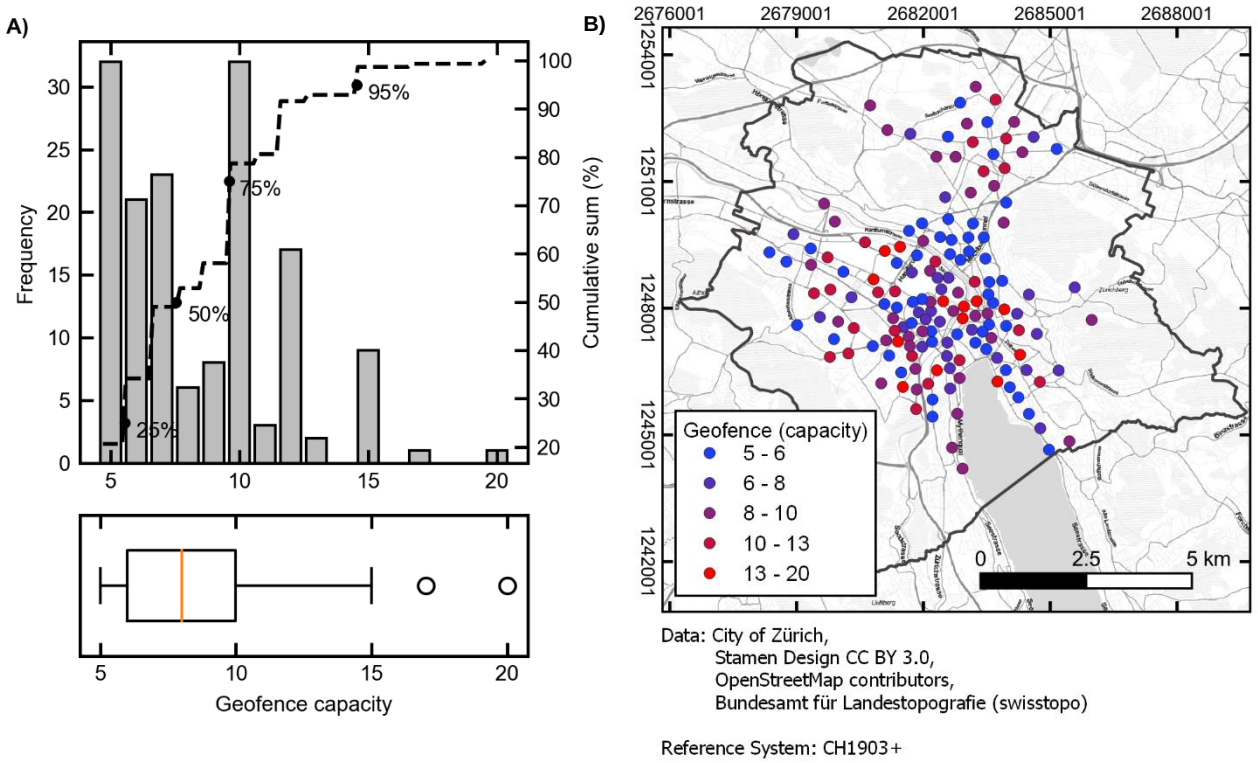

Figure 10. Bar chart of frequency of the various bicycle-capacities of the geofences proposed in the case study (A). The map shows the proposed geofences with the capacity color indicated by the color scheme (B).

The geofence evaluation over 1 hour intervals showed that the capacity was mostly sufficient to host the ODs occurring within the test cases areas. The numbers for each test case were computed for a 500 m radius around each OD that occurred within a time interval. The ratio difference between ODs and capacity had a mean of 32.4, indicating a general surplus of available capacity for the bike trips generated in the study area. 7% of the test cases had a negative difference of ODs and capacity meaning that not enough parking space was available in the 500 m radius.

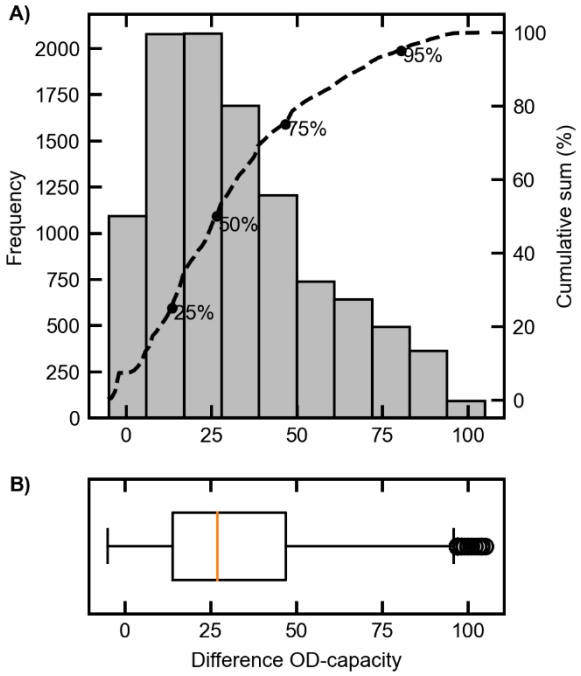

Figure 11. Distribution of difference between number of ODs and summed geofence capacity. The number of ODs was computed for a radius of 500 m around each OD that occurred within intervals of 1 hour.

5 Discussion

The growing implementation of dockless bike-sharing systems poses a challenge to many cities around the world. Due to the unrestricted nature of most dockless bike-sharing systems, improper parking behavior can lead to blocked sidewalks and vandalized bikes. Restricting the parking to geofences can help to solve this problem (Van Waes et al. 2018). The GIS-MCDA framework presented in this study can facilitate the selection of suitable, spatially well-distributed geofences for dockless shared bikes.

This study, similar to Kabak et al. (2018), used AHP to determine weights for the GIS-MCDA. This proved to be an efficient and structured method to combine the knowledge of different experts. In contrast to the study mentioned above, this framework implemented the AHP without holding a workshop where all experts would have to be present. Instead, a questionnaire was sent to each expert and the responses were aggregated afterward. This approach facilitated a fast and efficient implementation of the GIS-MCDA. Furthermore, holding a workshop requires the active presence of experts at a given time, an increase in effort that makes it more likely that fewer experts would be willing to participate in the study. The priority weights determined in the AHP indicate that the EDU and PTL criteria contribute the strongest to bike-sharing usage. They received weights of 0.23 and 0.21, respectively. COM, POP, and SP received lower values between 0.10 and 0.14. These findings are mostly consistent with the priority weights derived by Kabak et al. (2018), which compared mostly similar criteria. However, it is noteworthy that MBP, which received the lowest priority (0.04) in the results of this thesis, was ranked most influential in the previous study. This was most likely due to the different objectives of the studies. While Kabak et al. (2018) aimed to densify the existing sparse station network, which was exclusively built along a single major bike lane, this study aimed at creating a city-wide geofence network that not only covered bike lanes but also major parts of the study area.

Though there have been other publications proposing solutions for the planning of geofences for bike-sharing, the presented GIS-MCDA framework is, to the author's knowledge, the first approach to this issue to implement a method that does not rely on bike trip usage data. Other studies such as Cheng et al. (2019) and Zhang et al. (2019) determined geofence location mainly based on the micro-mobility data they acquired from bike-sharing businesses that have already been operational. The approach presented in this study, however, makes it possible to plan initial geofence locations for launching a fleet of dockless shared bikes in a new city. As the method mainly relies on free and globally-available data from OSM for the criteria representation and the network analysis, it can easily be adapted for new study areas. The exclusive use of free and open-source software facilitates this as well. It should be noted that geofence planning that uses bike trip data directly to select locations is likely to achieve better results than the presented GIS-MCDA, which uses criteria as proxies for bike-sharing usage. This approach should therefore be avoided for cities for which actual usage data is available.

Using existing infrastructure for the definition of candidate locations is an advantage of the approach of this study, especially compared to previous research which mostly assigned geofences or docking-stations to arbitrary places based solely on the modeled suitability (Conrow et al. 2018; Kabak et al. 2018; Cheng et al. 2019; Zhang et al. 2019). Due to the complexity of urban spaces, this is likely to result in a portion of the geofences or docking stations being at locations that are not suitable for this type of usage. Such locations could be on narrow sidewalks or places that are already used for other purposes. In contrast, using data of public bike parking as has been done in this study gives a high probability that the candidate location is at a place where there is space specifically dedicated for bike parking.

This study used VIKOR to rank the candidate locations according to their criteria scores. The resulting Qj measure that was used for the ranking exhibited a significant negative correlation with the frequency of ODs at a candidate location. This supports the assumption that the suitability derived by VIKOR in GIS-MCDA strongly relates to bike-sharing levels. The 10% and 90% percentiles that were used to define the threshold for highly suitable and unsuitable candidates should be evaluated for each application of the framework. The class of unsuitable locations is particularly relevant since these candidates will be excluded from further selection. In the case study, the 90% percentile was selected by visually examining the spatial distribution of the candidate locations. It was decided that by excluding the least suitable 10% a sufficient coverage could be achieved.

Comparing the results from the case study with the existing station-based bike-sharing system showed comparable coverage of the study area with a smaller number of locations. A total of 81% of the ODs were within 500 m network distance of at least one geofence. Related research indicates that a place that is within a distance smaller than 500 m to a bike-sharing facility is more likely to attract bike-sharing usage (Fuller et al. 2011; Tran et al. 2015). The mean distance of ODs to the closest geofence was 341 m which is 34 m shorter than for the existing stations. With this high proportion of ODs within a short distance to geofences, it can be assumed that most of the trips would have also been possible if the ODs were moved to geofences close by. The geofences also had better accessibility from the whole study area. This was reflected in the mean distance from any point in the road network to the closest geofence, which was 300 m shorter than the mean distance to the closest station within the existing bike-sharing station network.

Geofence capacity was determined based on suitability and available parking spots. This approach differs from other studies, where the capacity of geofences and stations was derived from demand and bike trip data (García-Palomares et al. 2012; Cheng et al. 2019; Zhang et al. 2019). Utilizing suitability instead of bike trip data makes this GIS-MCDA framework applicable to cities that lack such micro-mobility data. Taking the available bike racks at a geofence into account additionally ensures that the parking infrastructure is sufficient for the geofence capacity. In operational use of the proposed geofences, it will still be necessary to assess whether the capacity at the outer edge of the geofence network is sufficient. The total computed capacity of 1322 bikes would be adequate to host

the assumed fleet size of 600 bikes. The geofence network proposed in this study has a ratio of 2.2 between total capacity and fleet size. A search among different existing bike-sharing systems showed that a ratio of approximately 2.5 geofence or station spots per bike is common (e.g. Kaltenbrunner et al. 2010; Raviv and Kolka 2013). The comparison of demand and capacity over time showed that the geofences mostly have a sufficient capacity and a mean surplus of 32.4 parking spots. Only in 7% of the test cases was the demand not covered.

For the GIS-MCDA framework to produce good results, the priority weights derived by AHP must be meaningful. A prerequisite for this is that the definitions of the criteria are clear so that all experts understand them in the same way. If this is not the case, the pair-wise comparisons obtained from the experts cannot be combined and are practically meaningless. In this study, the ET criterion might not have been ideal as it combined different classes of sub-criteria. It included restaurants, theaters, and cinemas. These classes were combined with the assumption that they would attract similar types of bike rides. However, restaurants might contribute to bike-sharing levels at lunch and dinner time whereas theaters and cinemas are rather a contributor exclusively in the evenings. Additionally, people might be willing to cycle for longer distances to theaters and cinemas than to restaurants. However, it is generally not advisable to include a too large number of criteria in AHP. This rule is based on findings from cognitive science that humans have a working memory capacity of 7±2 (Saaty and Ozdemir 2003). Hence, the number of criteria in AHP preference judgments should be limited to a maximum of 9. This is why these criteria were pooled into super-classes. Future application of this framework should make sure to explain how the criteria are defined so that all experts base their pair-wise comparison on the same assumptions.

A limitation of the criteria layer creation is found in the density computation. The density of facilities was computed in a 2 km radius around a cell. This radius was derived from studies that showed that the majority of shared-bike trips are shorter than 2 km (Liu et al. 2018; Dong et al. 2019; Ma et al. 2020). However, this does not necessarily mean that all facilities in this buffer contribute to a location's suitability. A sensitivity analysis that investigates the effect of different buffer sizes could help to determine the adequate search radius for the density computation. Furthermore, the density computation utilized Euclidean distance, which might not be the most adequate distance for the urban space. For a more precise computation, network distance could be used. Since this would have resulted in cumbersome and time-consuming computations, this ultimately exceeded the scope of this study. Another aspect of the criteria layer creation that could be adjusted for future applications of the framework is the proximity computation of EDU. The computation did not distinguish between different types of buildings and campuses used for education. This might lead to bias in the result, as a single isolated institute cannot be expected to contribute in the same way to bike-sharing usage as a campus of a larger number of university buildings. To account for this it could be a solution to compute the number of buildings used for higher education within a specific distance of a cell instead of the distance to the closest such building.

In the location selection process, several candidate locations had to be discarded as they were located outside of the criteria layers. All of those candidates were located outside the buffer along the bike network. Investigating these cases revealed two different reasons for this. This was either because the location was in fact more than 10 m away from a bikeable street or because the bike network was incomplete. The bike network was retrieved from OSM, a system based on VGI that might not always cover the complete road network of a city. A recent study by Ferster et al. (2020) has shown that OSM has a high correlation in its bikeable road network as compared to public datasets. However, they state that OSM has issues with the tagging practice and that not all features in OSM are consistently tagged. This might have caused road segments to be left out from the network used in this study. A possible solution that would include more candidate locations would be to increase the buffer size. This would, however, lead to longer computation time.

The use of existing bike parking infrastructure as candidate locations was demonstrated to work well for the case study. This is especially valuable, given that datasets of parking infrastructure might not be available from official sources in all cities. OSM does include the tag "amenity=bicycle_parking" which is used to classify bike parking (OpenStreetMap Wiki 2021). It also offers a tag for capacity, which would make calculations for both location selection and capacity computation compatible with OSM data. However, considering the partly inconsistent nature of OSM tagging practices, future users of the GIS-MCDA framework should ensure that the data used to define the candidate locations has sufficient coverage and quality (Ferster et al. 2020). Additionally, it should be stated that the use of publicly funded infrastructure such as bike parking by a private company could be restricted by the local administration. For this reason, the capacity computation limited the maximum capacity to 50% of the available bike racks. This aimed to prevent conflict with other users of bike parking.

An aspect that has to be noted is that the bike trip data that was used to evaluate the selected geofence locations came from e-bikes. This might affect the trip data as e-bike users are more likely to commute for longer distances compared to users of regular bikes (Jahre et al. 2019). However, the fact that e-bike users cycle for longer distances does not mean they cycle to different destinations. The trip distance was also not considered in this study. It was therefore assumed that the contributing criteria of bike-sharing usage are similar for e-bikes and regular bikes. To further evaluate the proposed GIS-MCDA framework future research could aim at incorporating trip data from other non-electric dockless bike-sharing too.

The author sees the potential application of the presented GIS-MCDA framework primarily in the setting-up of geofence locations before the launch of a dockless bike-sharing system in a new service area. It can facilitate the prevention of improper parking behavior and can serve as an initial geofence network. The suitability map created in the framework can help to add additional geofences once the system is operational.

6 Conclusion

Following comprehensive literature research this study found explanatory factors that contribute to dockless bike-sharing levels, eight of which were selected for the GIS-MCDA. The factors that have the strongest impact according to the experts' assessment are institutions of higher education, large public transport stations, and entertainment facilities. It was demonstrated that the method developed in this study is capable of selecting suitable locations for the geofencing of dockless bike-sharing. Applying VIKOR suitability ranking for the location selection proved to work well as the closeness to the ideal solution measure computed by VIKOR revealed a significant negative correlation with bike trip frequency in a proximity to a geofence. The geofences proposed for the case study had an equivalent coverage to the existing station network while demanding a lower number of locations. Looking at the entire study area, the geofences have the potential to serve an even larger service area than the existing stations as they have a shorter average distance to points in the road network. The geofence capacity determination presented in this study differs from previous approaches, in that it takes the existing bike parking infrastructure into account and limits the geofence capacity to avoid blocking all available parking spots. This ensures selecting locations that are designated for bike parking. The capacity computed in the case study was found to be able to cover 93% of the demand in the case study.

References

Aczél, J., and T. L. Saaty. 1983. Procedures for synthesizing ratio judgements. *Journal of Mathematical Psychology* 27: 93–102. doi:10.1016/0022-2496(83)90028-7.

Alonso, J. A., and M. T. Lamata. 2006. Consistency in the analytic hierarchy process: a new approach. *International Journal of Uncertainty, Fuzziness and Knowledge-Based Systems* 14: 445–459. doi:10.1142/S0218488506004114.

Boeing, G. 2017. OSMnx: New methods for acquiring, constructing, analyzing, and visualizing complex street networks. *Computers, Environment and Urban Systems* 65: 126–139. doi:10.1016/j.compenvurbsys.2017.05.004.

BOND Mobility AG. 2020. BOND erweitert Betriebsgebiet auf ganze Stadt Zürich. Press release. Zürich.

Brunelli, M. 2015. *Introduction to the Analytic Hierarchy Process*. SpringerBriefs in Operations Research. Cham: Springer International Publishing. doi:10.1007/978-3-319-12502-2.

Buehler, R., and J. Pucher. 2012. Cycling to work in 90 large American cities: new evidence on the role of bike paths and lanes. *Transportation* 39: 409–432. doi:10.1007/s11116-011-9355-8.

Bundesamt für Statistik. 2020. *Statistik der Bevölkerung und Haushalte (STATPOP), Geodaten 2019*. 14716365. Neuchâtel: BFS.

Butler, G. P., H. M. Orpana, and A. J. Wiens. 2007. By Your Own Two Feet. *Canadian Journal of Public Health* 98: 259–264. doi:10.1007/BF03405399.

Cheng, E. W. L., and H. Li. 2001. Analytic hierarchy process: an approach to determine measures for business performance. *Measuring Business Excellence* 5. MCB UP Ltd: 30–37. doi:10.1108/EUM0000000005864.

Cheng, G., Y. Guo, Y. Chen, and Y. Qin. 2019. Designating City-Wide Collaborative Geofence Sites for Renting and Returning Dock-Less Shared Bikes. *Ieee Access* 7. Piscataway: Ieee-Inst Electrical Electronics Engineers Inc: 35596–35605. doi:10.1109/ACCESS.2019.2903521.

Conrow, L., A. T. Murray, and H. A. Fischer. 2018. An optimization approach for equitable bicycle share station siting. *Journal of Transport Geography* 69: 163–170. doi:10.1016/j.jtrangeo.2018.04.023.

Daim, T. U., A. Udbye, and A. Balasubramanian. 2013. Use of analytic hierarchy process (AHP) for selection of 3PL providers. *Journal of Manufacturing Technology Management* 24. Emerald Group Publishing Limited: 28–51. doi:10.1108/17410381311287472.

DeMaio, P. 2009. Bike-sharing: History, Impacts, Models of Provision, and Future. *Journal of Public Transportation* 12. doi:http://doi.org/10.5038/2375-0901.12.4.3.

Dill, J., and T. Carr. 2003. Bicycle Commuting and Facilities in Major U.S. Cities: If You Build Them, Commuters Will Use Them. *Transportation Research Record* 1828. SAGE Publications Inc: 116–123. doi:10.3141/1828-14.

Dong, J., B. Chen, L. He, C. Ai, F. Zhang, D. Guo, and X. Qiu. 2019. A Spatio-Temporal Flow Model of Urban Dockless Shared Bikes Based on Points of Interest Clustering. *ISPRS International Journal of Geo-Information* 8. Multidisciplinary Digital Publishing Institute: 345. doi:10.3390/ijgi8080345.

Eastman, J. R., P. Kyem, J. Toledano, and W. Jin. 1993. GIS and decision making. *The Clarks Labs for Cartographic Technology and Geographic Analysis.*

Eren, E., and V. E. Uz. 2020. A review on bike-sharing: The factors affecting bike-sharing demand. *Sustainable Cities and Society* 54: 101882. doi:10.1016/j.scs.2019.101882.

Faghih-Imani, A., and N. Eluru. 2015. Analysing bicycle-sharing system user destination choice preferences: Chicago's Divvy system. *Journal of Transport Geography* 44: 53–64. doi:10.1016/j.jtrangeo.2015.03.005.

Faghih-Imani, A., N. Eluru, A. M. El-Geneidy, M. Rabbat, and U. Haq. 2014. How land-use and urban form impact bicycle flows: evidence from the bicycle-sharing system (BIXI) in Montreal. *Journal of Transport Geography* 41: 306–314. doi:10.1016/j.jtrangeo.2014.01.013.

Ferster, C., J. Fischer, K. Manaugh, T. Nelson, and M. Winters. 2020. Using OpenStreetMap to inventory bicycle infrastructure: A comparison with open data from cities. *International Journal of Sustainable Transportation* 14. Taylor & Francis: 64–73. doi:10.1080/15568318.2018.1519746.

Frade, I., and A. Ribeiro. 2015. Bike-sharing stations: A maximal covering location approach. *Transportation Research Part A: Policy and Practice* 82: 216–227. doi:10.1016/j.tra.2015.09.014.

Fuller, D., L. Gauvin, Y. Kestens, M. Daniel, M. Fournier, P. Morency, and L. Drouin. 2011. Use of a New Public Bicycle Share Program in Montreal, Canada. *American Journal of Preventive Medicine* 41: 80–83. doi:10.1016/j.amepre.2011.03.002.

García-Palomares, J. C., J. Gutiérrez, and M. Latorre. 2012. Optimizing the location of stations in bike-sharing programs: A GIS approach. *Applied Geography* 35: 235–246. doi:10.1016/j.apgeog.2012.07.002.

Gillies, S. 2019. *Rasterio: geospatial raster I/O for {Python} programmers*. Mapbox.

Goodchild, M. F. 2007. Citizens as sensors: the world of volunteered geography. *GeoJournal* 69: 211–221. doi:10.1007/s10708-007-9111-y.

Guitouni, A., and J.-M. Martel. 1998. Tentative guidelines to help choosing an appropriate MCDA method. *European Journal of Operational Research* 109: 501–521. doi:10.1016/S0377-2217(98)00073-3.

Harris, C. R., K. J. Millman, S. J. van der Walt, R. Gommers, P. Virtanen, D. Cournapeau, E. Wieser, J. Taylor, et al. 2020. Array programming with NumPy. *Nature* 585: 357–362. doi:10.1038/s41586-020-2649-2.

Hirsch, J. A., J. Stratton-Rayner, M. Winters, J. Stehlin, K. Hosford, and S. J. Mooney. 2019. Roadmap for free-floating bikeshare research and practice in North America. *Transport reviews* 39: 706–732. doi:10.1080/01441647.2019.1649318.

Hwang, C.-L., and K. Yoon. 1981. Methods for Multiple Attribute Decision Making. In *Multiple Attribute Decision Making: Methods and Applications A State-of-the-Art Survey*, ed. C.-L. Hwang and K. Yoon, 58–191. Lecture Notes in Economics and Mathematical Systems. Berlin, Heidelberg: Springer. doi:10.1007/978-3-642-48318-9_3.

Jahre, A. B., E. Bere, S. Nordengen, A. Solbraa, L. B. Andersen, A. Riiser, and H. B. Bjørnarå. 2019. Public employees in South-Western Norway using an e-bike or a regular bike for commuting – A cross-sectional comparison on sociodemographic factors, commuting frequency and commuting distance. *Preventive Medicine Reports* 14: 100881. doi:10.1016/j.pmedr.2019.100881.

Jiang, H., and J. R. Eastman. 2000. Application of fuzzy measures in multi-criteria evaluation in GIS. *International Journal of Geographical Information Science* 14. Taylor & Francis: 173–184. doi:10.1080/136588100240903.

Jordahl, K., J. V. D. Bossche, M. Fleischmann, J. McBride, J. Wasserman, J. Gerard, A. G. Badaracco, A. D. Snow, et al. 2021. *geopandas/geopandas: v0.8.2* (version v0.8.2). Zenodo. doi:10.5281/ZENODO.4464949.

Kabak, M., M. Erbaş, C. Çetinkaya, and E. Özceylan. 2018. A GIS-based MCDM approach for the evaluation of bike-share stations. *Journal of Cleaner Production* 201: 49–60. doi:10.1016/j.jclepro.2018.08.033.

Kabir, G., R. Sadiq, and S. Tesfamariam. 2014. A review of multi-criteria decision-making methods for infrastructure management. *Structure and Infrastructure Engineering* 10: 1176–1210. doi:10.1080/15732479.2013.795978.

Kaltenbrunner, A., R. Meza, J. Grivolla, J. Codina, and R. Banchs. 2010. Urban cycles and mobility patterns: Exploring and predicting trends in a bicycle-based public transport system. *Pervasive and Mobile Computing* 6. Human Behavior in Ubiquitous Environments: Modeling of Human Mobility Patterns: 455–466. doi:10.1016/j.pmcj.2010.07.002.

Keeney, R. L. 1992. *Value-focused thinking: a path to creative decisionmaking*. Cambridge, Mass.: Harvard Univ. Press.

Krizek, K. J., and P. J. Johnson. 2006. Proximity to Trails and Retail: Effects on Urban Cycling and Walking. *Journal of the American Planning Association* 72. Routledge: 33–42. doi:10.1080/01944360608976722.

Li, A., P. Zhao, Y. Huang, K. Gao, and K. W. Axhausen. 2020. An empirical analysis of dockless bike-sharing utilization and its explanatory factors: Case study from Shanghai, China. *Journal of Transport Geography* 88: 102828. doi:10.1016/j.jtrangeo.2020.102828.

Liu, Z., Y. Shen, and Y. Zhu. 2018. Inferring Dockless Shared Bike Distribution in New Cities. In *Proceedings of the Eleventh ACM International Conference on Web Search and Data Mining*, 378–386. WSDM '18. New York, NY, USA: Association for Computing Machinery. doi:10.1145/3159652.3159708.

Ma, X., Y. Ji, Y. Yuan, N. Van Oort, Y. Jin, and S. Hoogendoorn. 2020. A comparison in travel patterns and determinants of user demand between docked and dockless bike-sharing systems using multi-sourced data. *Transportation Research Part A: Policy and Practice* 139: 148–173. doi:10.1016/j.tra.2020.06.022.

Malczewski, J. 2006. GIS-based multicriteria decision analysis: a survey of the literature. *International Journal of Geographical Information Science* 20. Taylor & Francis: 703–726. doi:10.1080/13658810600661508.

Martin, E. W., and S. A. Shaheen. 2014. Evaluating public transit modal shift dynamics in response to bikesharing: a tale of two U.S. cities. *Journal of Transport Geography* 41: 315–324. doi:10.1016/j.jtrangeo.2014.06.026.

McKenzie, G. 2018. Docked vs. Dockless Bike-sharing: Contrasting Spatiotemporal Patterns (Short Paper). In *10th International Conference on Geographic Information Science (GIScience 2018)*, ed. S. Winter, A. Griffin, and M. Sester, 114:46:1-46:7. Leibniz International Proceedings in Informatics (LIPIcs). Dagstuhl, Germany: Schloss Dagstuhl–Leibniz-Zentrum fuer Informatik. doi:10.4230/LIPIcs.GISCIENCE.2018.46.

Neutron Holdings, Inc. 2017. LimeBike Celebrate's 1,000,000th Ride With European Expansion. Press release.

OpenStreetMap contributors. 2021. OpenStreetMap.

OpenStreetMap Wiki. 2020. Tags — OpenStreetMap Wiki.

OpenStreetMap Wiki. 2021. Tag:amenity=bicycle parking — OpenStreetMap Wiki.

Opricovic, S., and G. H. Tzeng. 2004. Compromise solution by MCDM methods: A comparative analysis of VIKOR and TOPSIS. *European Journal of Operational Research* 156. Amsterdam: Elsevier: 445–455. doi:10.1016/s0377-2217(03)00020-1.

Pal, A., and Y. Zhang. 2017. Free-floating bike sharing: Solving real-life large-scale static rebalancing problems. *Transportation Research Part C: Emerging Technologies* 80: 92–116. doi:10.1016/j.trc.2017.03.016.

Pereira, J. M., and L. Duckstein. 1993. A multiple criteria decision-making approach to GIS-based land suitability evaluation. *International journal of geographical Information science* 7. Taylor & Francis: 407–424.

PubliBike AG. 2018. Wir feiern die Eröffnung von «Züri Velo»! Press release.

Ramanathan, R. 2001. A note on the use of the analytic hierarchy process for environmental impact assessment. *Journal of Environmental Management* 63: 27–35. doi:10.1006/jema.2001.0455.

Raviv, T., and O. Kolka. 2013. Optimal inventory management of a bike-sharing station. *IIE Transactions* 45. Taylor & Francis: 1077–1093. doi:10.1080/0740817X.2013.770186.

Reclus, F., and K. Drouard. 2009. Geofencing for fleet freight management. In *2009 9th International Conference on Intelligent Transport Systems Telecommunications, (ITST)*, 353–356. doi:10.1109/ITST.2009.5399328.

Saaty, T. L. 1980. *The analytic hierarchy process*. Edited by Roman Słowiński. McGraw-Hill International Book Co., New York.

Saaty, T. L., and M. S. Ozdemir. 2003. Why the magic number seven plus or minus two. *Mathematical and Computer Modelling* 38: 233–244. doi:10.1016/S0895-7177(03)90083-5.

Sanchez-Lozano, J. M., M. S. Garcia-Cascales, and M. T. Lamata. 2016. GIS-based onshore wind farm site selection using Fuzzy Multi-Criteria Decision Making methods. Evaluating the case of Southeastern Spain. *Applied Energy* 171. Oxford: Elsevier Sci Ltd: 86–102. doi:10.1016/j.apenergy.2016.03.030.

Shen, Y., X. Zhang, and J. Zhao. 2018. Understanding the usage of dockless bike sharing in Singapore. *International Journal of Sustainable Transportation* 12. Taylor & Francis: 686–700. doi:10.1080/15568318.2018.1429696.

Shui, C. S., and W. Y. Szeto. 2020. A review of bicycle-sharing service planning problems. *Transportation Research Part C: Emerging Technologies* 117: 102648. doi:10.1016/j.trc.2020.102648.

Sirikrai, S. B., and J. C. S. Tang. 2006. Industrial competitiveness analysis: Using the analytic hierarchy process. *The Journal of High Technology Management Research* 17: 71–83. doi:10.1016/j.hitech.2006.05.005.

Stadt Zürich. 2021. Zürich in Zahlen. https://www.stadt-zuerich.ch/portal/de/index/portraet_der_stadt_zuerich/zuerich_in_zahlen.html. Accessed January 27.

Stadtrat Zürich, ed. 2012. Masterplan Velo.

Statistik Stadt Zürich. 2021. Bevölkerungsszenarien 2020. https://www.stadt-zuerich.ch/prd/de/index/statistik/kontakt-medien/aktuell/neuigkeiten/2020/2020-04-28_Bevoelkerungsszenarien.html. Accessed January 27.

Tran, T. D., Nicolas Ovtracht, and Bruno Faivre d'Arcier. 2015. Modeling Bike Sharing System using Built Environment Factors. *Procedia CIRP* 30. Elsevier: 293–298. doi:10.1016/j.procir.2015.02.156.

Van Rossum, G., and F. L. Drake. 2009. *The Python language reference*. Release 3.0.1 [Repr.]. Python Documentation Manual Guido van Rossum; Fred L. Drake [ed.] ; Pt. 2. Hampton, NH: Python Software Foundation.

Van Waes, A., J. Farla, K. Frenken, J. P. J. de Jong, and R. Raven. 2018. Business model innovation and socio-technical transitions. A new prospective framework with an application to bike sharing. *Journal of Cleaner Production* 195: 1300–1312. doi:10.1016/j.jclepro.2018.05.223.

Wang, K., G. Akar, and Y.-J. Chen. 2018. Bike sharing differences among Millennials, Gen Xers, and Baby Boomers: Lessons learnt from New York City's bike share. *Transportation Research Part A: Policy and Practice* 116: 1–14. doi:10.1016/j.tra.2018.06.001.

Wątróbski, J., J. Jankowski, P. Ziemba, A. Karczmarczyk, and M. Zioło. 2019. Generalised framework for multi-criteria method selection. *Omega* 86: 107–124. doi:10.1016/j.omega.2018.07.004.

Zhang, Y., D. Lin, and Z. Mi. 2019. Electric fence planning for dockless bike-sharing services. *Journal of Cleaner Production* 206. Elsevier: 383–393. doi:10.1016/j.jclepro.2018.09.215.